AGU PUBLICATIONS

JGR

Journal of Geophysical Research: Oceans

RESEARCH ARTICLE

10.1002/2014JC009972

Evidence of Mediterranean Water dipole collision in the Gulf of Cadiz

Pierre L'Hégaret[1], Xavier Carton[1], Isabel Ambar[2], Claire Ménesguen[1], Bach Lien Hua[1,3], Laurent Chérubin[4], Ana Aguiar[5], Bernard Le Cann[1], Nathalie Daniault[1], and Nuno Serra[6]

[1]LPO, UBO/UEB and IFREMER, Brest, France, [2]Centro de Oceanografia, University of Lisbon, Lisbon, Portugal, [3]Deceased 27 November 2012, [4]HBOI, Florida Atlantic University, Fort Pierce, Florida, USA, [5]Instituto Dom Luiz, University of Lisbon, Lisbon, Portugal, [6]Institut fur Meereskunde, University of Hamburg, Hamburg, Germany

Key Points:
- Observations of the collision of Mediterranean dipole eddies in the Gulf of Cadiz
- Following the merger of those eddies and registering of the result
- We followed a meddy for over a year and its interactions with other eddies

Correspondence to:
P. L'Hégaret,
pierre.lhegaret@univ-brest.fr

Citation:
L'Hégaret, P., X. Carton, I. Ambar, C. Ménesguen, B. L. Hua, L. Chérubin, A. Aguiar, B. Le Cann, N. Daniault, and N. Serra (2014), Evidence of Mediterranean Water dipole collision in the Gulf of Cadiz, *J. Geophys. Res. Oceans*, *119*, doi:10.1002/2014JC009972.

Received 14 MAR 2014
Accepted 10 JUL 2014
Accepted article online 15 JUL 2014

Abstract A collision of Mediterranean Water dipoles in the Gulf of Cadiz is studied here, using data from the MedTop and Semane experiments. First, a Mediterranean Water eddy (meddy) was surveyed hydrologically in November 2000 southwest of Cape Saint Vincent. Then, this meddy drifted northeastward from this position, accompanied by a cyclone (detected only via altimetry), thus forming a first dipole. In February 2001, a dipole of Mediterranean Water was measured hydrologically just after its formation near Portimão Canyon. This second dipole drifted southwestward. The western and eastern meddies had hydrological radii of about 22 and 25 km, respectively, with corresponding temperature and salinity maxima of (13.45°C, 36.78) and (11.40°C, 36.40). Rafos float trajectories and satellite altimetry indicate that these two dipoles collided early April 2001, south of Cape Saint Vincent, near 35°30′N, 10°15′W. More precisely, the eastern meddy wrapped around the western one. This merger resulted in an anticyclone (a meddy) which drifted southeastward, coupled with the eastern cyclone. Hydrological sections across this final third resulting dipole, performed in July 2001 in the southern Gulf of Cadiz, confirm this interaction: the thermohaline characteristics of the final meddy can be tracked back to the original structures. The subsequent evolution of this dipole was analyzed with Rafos float trajectories. A numerical simulation of the interaction between the two earlier dipoles is also presented. We suggest that these dipole collisions at the Mediterranean Water level may represent a mechanism of generation of the larger meddies that finally leave the Gulf of Cadiz.

1. Introduction

In the Straits of Gibraltar, fresher north Atlantic water enters the Mediterranean Sea near the surface, and saltier Mediterranean Water flows westward near the bottom. This outflow of Mediterranean Water cascades down on the continental slope of the Gulf of Cadiz, mixes with surrounding north Atlantic Central Water, and veers northward under the influence of the Coriolis force. This Mediterranean Water (MW) forms several cores of mixed water, which stabilize at depths of 400, 800, and 1200 m (called, respectively, the coastal or shallow, upper, and lower cores of MW) [*Madelain*, 1970; *Zenk*, 1975; *Ambar*, 1983]. These cores follow the Iberian continental slope northwestward. Crossing the Portimão Canyon (near 8°30′W, 36°30′N) and then the Cape Saint Vincent canyon (near 9°30′W), the upper and lower cores of MW are destabilized and form mesoscale lenses, called MW cyclones and meddies [MW anticyclones; see in particular *Armi and Zenk*, 1984; *Armi et al*., 1989; *Prater and Sanford*, 1994; *Bower et al*., 1995, 1997; *Sadoux et al*., 2000; *Chérubin et al*., 2000; *Serra and Ambar*, 2002; *Serra et al*., 2005; *Ambar et al*., 2008]. Several sites of meddy formation have been identified along the west coast of Portugal and Spain notably: the Estremadura Promontory [*Käse et al*., 1989; *Zenk et al*., 1992] and Cape Ortegal [*Paillet et al*., 1999, 2002].

Meddies are biconvex, anticyclonic lenses of MW with radii of 20–75 km, thicknesses of 500–1000 m, centered at 1000 m depth, and azimuthal velocities of 0.2–0.5 m s^{-1} [*Bower*, 1994; *Richardson et al*., 2000]. They contain warm and salty waters usually with a temperature maximum near 800 m depth and a salinity maximum near 1200 m depth. The average direction of meddy propagation, under the influence of beta effect, currents and topography, is southwestward [*Colin de Verdière*, 1992; *Daniault et al*., 1994], but many deviations from this direction have been observed [*Käse and Zenk*, 1986; *Shapiro and Meschanov*, 1996; *Richardson et al*., 1989, 1991, 2000; *Richardson and Tychensky*, 1998; *Tychensky and Carton*, 1998; *Paillet et al*., 1999, 2002; *Carton et al*., 2010; *Barbosa Aguiar et al*., 2013].

In *Carton et al*. [2010], the evolution of two meddies, detected and sampled southwest of Cape Saint Vincent in November 2000, was reported. These meddies interacted briefly and then followed different trajectories. The easternmost meddy coupled with a cyclone located on its southern side and drifted westward (as revealed by the analysis of altimetric maps). The westernmost meddy followed an unusual Y-shaped trajectory revealed by the tracking of Rafos floats seeded and trapped in this eddy. The first part of this trajectory resulted a priori from the coupling of the westernmost meddy with a cyclone initially located on its northern flank. The second part of this trajectory was interpreted as the coupling of this meddy with another cyclone coming from the northeastern Gulf of Cadiz.

In this paper, we analyze these eddies in detail. By joining two observational databases and satellite data, we have been able to identify the origin and structure of the latter cyclone: originally it was part of the dipole first located near Portimão Canyon. We describe the initial state of these dipoles, positions and hydrological characteristics, in November 2000 for the westernmost dipole, in February 2001 for the easternmost, Portimão, dipole, and then in June 2001 for the final dipole. These latter hydrological sections shed light on the origin of the water masses that this final dipole contained. We then compare the trajectories of the Rafos floats initially seeded in the two original meddies, providing evidence of a strong interaction between these two meddies. We also compare Sea Level Anomalies (SLA) and Sea Surface Temperature (SST) evolution with the trajectories of the floats. Finally, other Rafos float trajectories in the vicinity of these dipoles indicate the presence and evolution of other eddies in the Gulf of Cadiz at the same period. To confirm our hypothesis, we ran idealized simulations of meddy or deep eddy collisions. We compared their results with those of experimental studies of collisions of two dipoles [*Van Heijst and Flor*, 1989].

2. Data and Methods

2.1. Data Collection

The MedTop program, directed by the Centro de Oceanografia of the University of Lisbon, was designed to understand the role of bottom topography, and in particular of the Portimão Canyon, in the generation and further evolution of meddies and MW cyclones. This program carried out three experiments at sea in February, May, and September 2001. Five hydrological sections, with XBT casts and CTD stations closely spaced (five nautical miles, NM) on each section, were performed during each cruise (see Figure 1). Whenever such eddies were detected, Rafos floats were seeded in them. Results from the Meddy program can be found in *Serra et al*. [2005], *Ambar et al*. [2008], and *Serra et al*. [2010].

The Semane program, directed by the French Navy Oceanographic Service of Brest, was designed to understand the structure and variability of the MW cores and of detached eddies in the Gulf of Cadiz. This program carried out seven experiments at sea in November 1995, July 1997, July 1999, July 2000, November 2000, July 2001, and July 2002 (the latter experiment was carried out by IFREMER). Long CTD-LADCP sections across the Gulf were performed during these cruises and the results are described in other papers [*Quentel et al*., 2011; *Alves et al*., 2011]. These experiments also included XBT-XCTD cross sections of eddies, previously detected by altimetry or via other hydrological sections. Rafos floats, or deep-drogued Surdrift buoys, were also released in such eddies [see, for instance, *Carton et al*., 2002]. The XBT-XCTD casts of interest from Semane in November 2000 and June 2001 are shown on map (Figure 1).

For comparison with hydrological data, we used monthly mean fields of SLA obtained from AVISO with a 1/4 $\times$ 1/4° resolution on a Mercator grid and a daily interpolation. Informations and data sets can be retrieved from: http://www.aviso.altimetry.fr/en/data/products.html. Level 4, monthly averaged, SST maps with a 1/4 $\times$ 1/4° resolution were obtained from the Met Office Ostia system. Data can be retrieved from: http://www.ncof.co.uk/. SST anomalies were calculated from the 23 year climatology. Finally, topographic maps were obtained from the NGDC data center ETOPO1.

2.2. Data Processing

Hydrological profiles performed during these cruises measured temperature and salinity from surface to bottom (salinity was calibrated via chemical analysis of water samples conductivity and temperature). Visual analysis of each profile, and a median filter eliminated spurious points on the profiles. Then a binomial Newtonian smoothing was applied to reduce the number of points to 10 or 20% of the initial number, under the condition that the initial profile could be reconstructed from the final one with an error at most equal to the probe

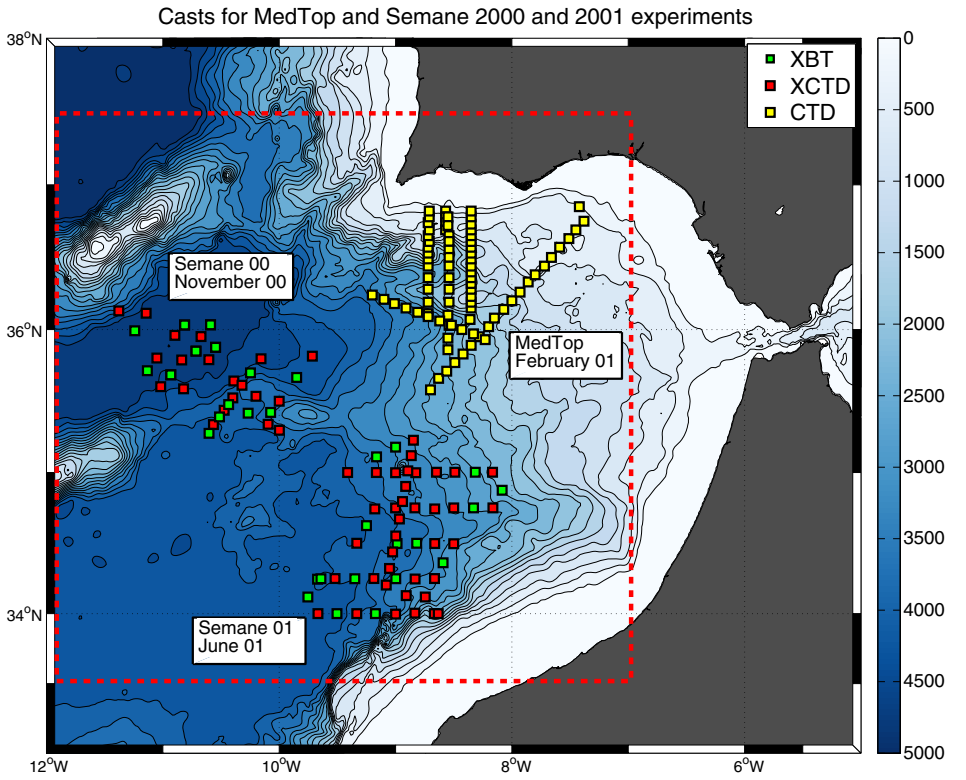

Figure 1. Hydrological sections of the MedTop and Semane experiments superimposed on bathymetry; XBT, XCTD, and CTD casts are indicated in green, red, and yellow.

accuracy. With XBTs and XCTDs, the accuracy on temperature measurements is 0.018°C and that on salinity is 0.013 (the same accuracy is obtained for reconstructed salinity profiles). From a water mass diagram, salinity was reconstructed for XBTs using the method developed by *Käse et al.* [1996]. In Figure 1, we note that the XBT and XCTD casts were performed very closely. In order to calculate a regression of salinity on the locations of the XBT probes, we used the XTCD data. We plotted T-S diagram and inferred the properties of the MW and the surrounding waters. Those hydrological properties varying smoothly from one water mass to another, we could obtain salinity profiles associated with the temperature measured via XBT.

Many isobaric Rafos floats were released during the Semane and MedTop experiments, but we will only present here the trajectories of three floats. Float SV106 (renamed RF1 hereafter) was released in the northwestern meddy identified and sampled on 28 November 2000, at 35°36.40′N– 10°19.19′W; this float was ballasted at 1000 dbar. Float me203 (RF2 hereafter) was released in a meddy at 36°08.46′N–8°55.45′W on 28 February 2001; it was ballasted at 1300 dbar. Float me206 (hereafter RF3) was released at 36°11.24′N–8°02.28′W on 23 February 2001; it was also ballasted at 1300 dbar. These floats were located by sound sources, a Portuguese source and two German sources (a distant source in the north Atlantic was used in case of ambiguities on the trajectories). Absolute precision of the positioning is 5 km, obtained as the distance between the last acoustic triangulation and the first surface location given by ARGOS, but relative errors within a trajectory are likely to be smaller.

Deep-drogued Surdrift buoys were released during Semane 2001. A 10 m long holeysock drogue was tethered to the surface buoy by a 2 mm thick Kevlar cable. These cables were 900–1200 m long. All Surdrift buoys were programmed for a 180 day mission and positioned via ARGOS.

3. Analysis of the Experiments Data Showing the Eddy Interaction

3.1. Presentation of Dipoles and Summary of Their Interactions

First of all, we present here the known positions and evolutions of meddies and cyclones at three different periods: in November 2000, February and June 2001, during Semane 2000, MedTop and Semane 2001,

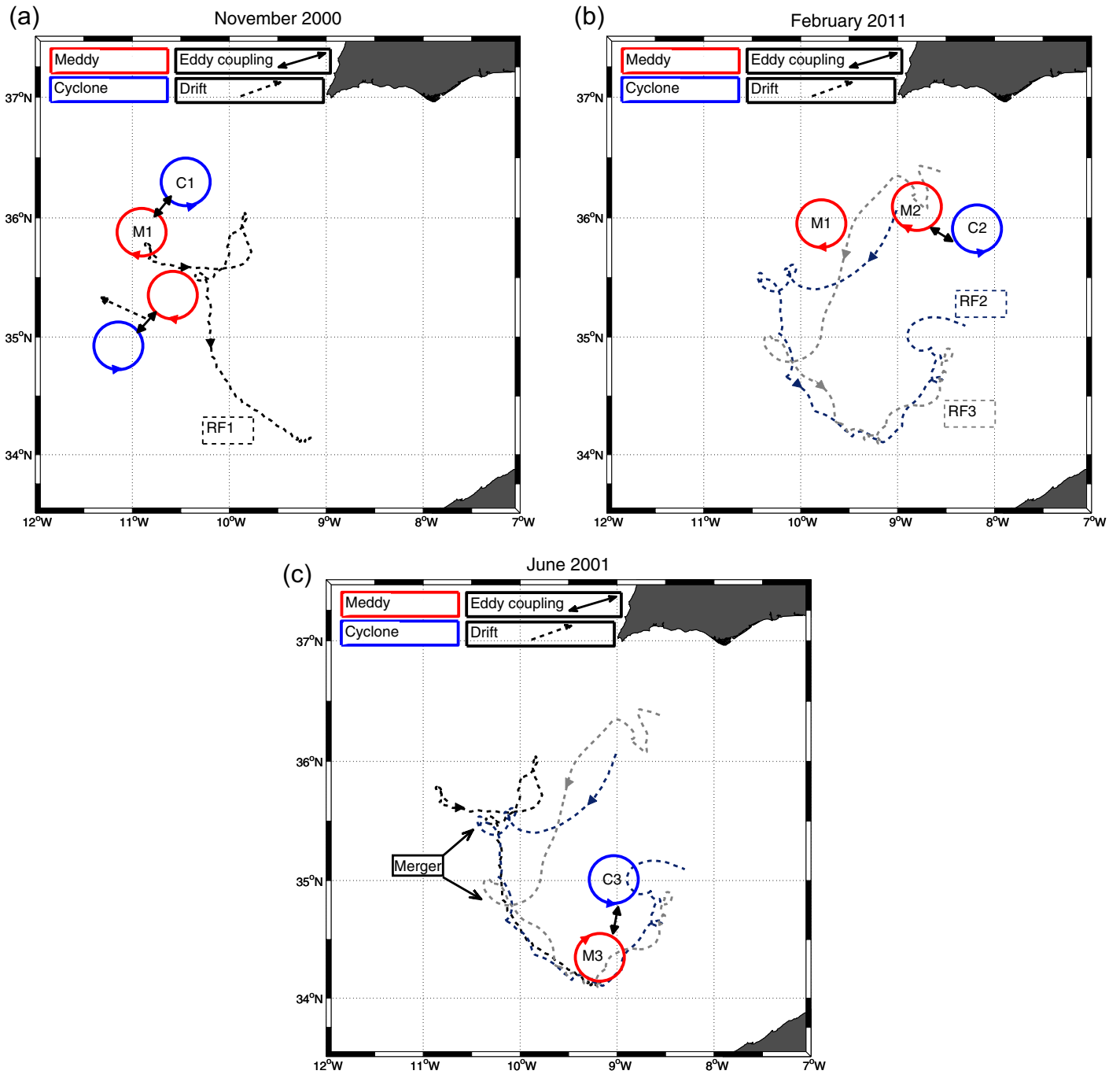

Figure 2. Sketches of the positions of the eddies at different times (a) in November 2000 with M1-C1 and RF1 drift (b) in February 2001 with M2-C2 and M1 relative position, and RF2, RF3 drifts, and (c) in June 2001 with M3-C3 with the previous drifts (RF1, RF2, and RF3).

respectively (Table 1). Their thermohaline and dynamical characteristics, as well as their surface signatures will be described chronologically in the following sections. During the Semane 2000 experiment which took place in November 2000, two dipoles were identified by *Carton et al.* [2010] southwest of Cape Saint Vincent. The meddies were, respectively, located near 35°45′N, 10°75′W and 35°30′N, 10°15′W (see Figure 2a, for positions). They were accompanied by two cyclones detected on altimetry by pronounced depressions north and south of the meddies, respectively. For this study, we will focus on the northern dipole and refer to the meddy and the cyclone as M1 and C1. Furthermore, a Rafos float, RF1, was trapped in M1 for 9 months,

Table 1. Table of Eddies Names, Period of First Measurement, Drifts, Interactions, and Floats

Eddy	First Measure	Drift	Interaction	Floats
M1	November 2000	East	Merged with M2	RF1
C1	November 2000 (via altimetry)	East	Interacted with C2	None
M2	February 2001	Southwest	Merged with M1	RF2 and RF3 from April
C2	February 2001	Southwest	Interacted with C1	None
M3	June 2001	Rotates around C3	Results from the merging of M1 and M2	SF
C3	June 2001	Stationary from April to June		None

the recorded temperature did not vary substantially; we will use it here as a marker of this meddy (see Figure 2a, the drift of the meddy center, calculated from the RF1 position records as in *Paillet et al.* [1999]).

In February 2001, hydrological sections from the MedTop experiment revealed another dipole southwest of Portimão Canyon. The meddy was centered near 36°N, 8°45′W and the cyclone near 36°N, 8°15′W (see Figure 2b). We will call them M2 and C2, respectively. Two Rafos floats, RF2 and RF3 followed M2 from February to September and April to September, respectively.

Finally, in June 2001, a third dipole was detected from Semane 2001 hydrological sections, with a meddy near 34°15′N, 9°30′W and a cyclone north of it at 35°N, 9°W (see Figure 2c). The three Rafos floats described earlier were found around this meddy and a Surdrift buoy (SF) was released inside it. Our assumption is that the first two dipoles (M1-C1 and M2-C2) collided and that the meddies merged to form M3.

3.2. Hydrographic, Dynamical Characteristics, and Drifts of the Dipoles

3.2.1. Meddy Southwest of Cape Saint Vincent in November 2000, M1

The hydrological sections from Semane 2000 in November 2000 measured M1. It had a double core structure with a temperature maximum of 13.4°C near 700 m depth, and a salinity maximum of 36.8 near

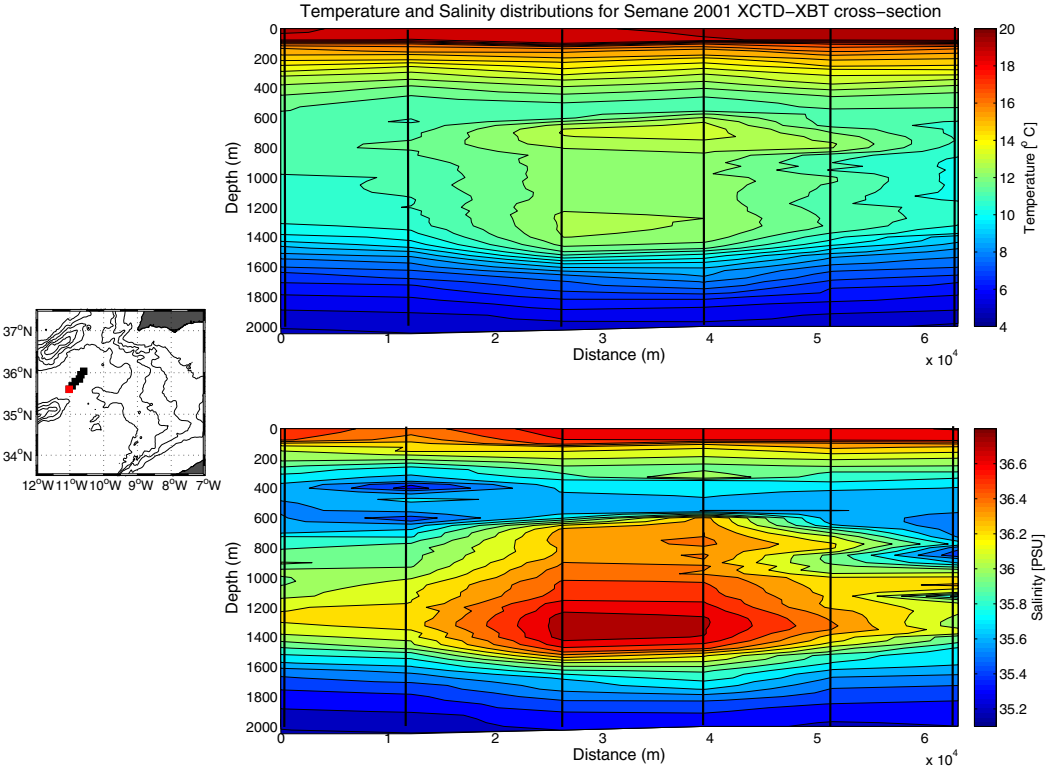

Figure 3. Temperature and salinity section of the meddy M1 of Semane 2000 (November 2000) at its initial position near 35°N and 11°W [from *Carton et al.*, 2010]. The distance is measured from the beginning of the section at its southwesternmost point. This anticyclone has two cores, one with a temperature maximum 13.4°C near 700 m depth, and one with a salinity maximum of 36.8 near 1300 m.

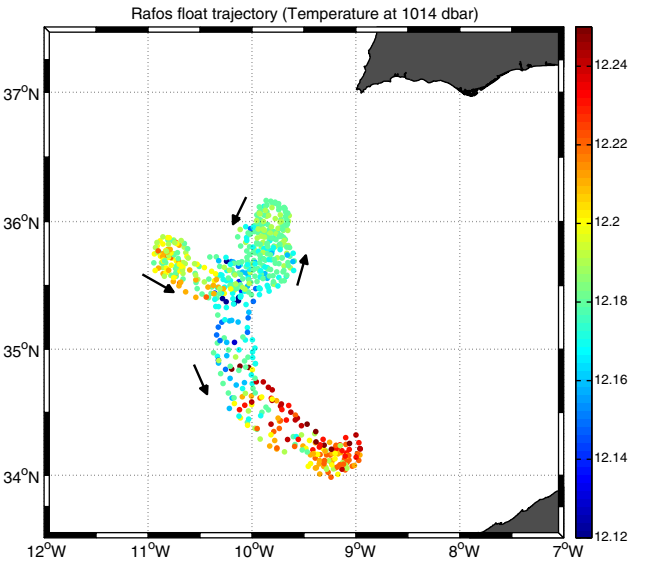

Figure 4. Trajectories of Rafos float RF1 of Semane 2000 program starting on November 2000 on the northwest, colored by temperature. Temperature and distance to the meddy center (M1) of RF1 vary very little during the 9 months of record.

1300 m. The double core structure and these thermohaline maxima are characteristics of a meddy formed near the Portimão Canyon [*Chérubin et al*., 2000]. Its hydrological radius, based on isotherm 11.5°C (or isohaline 36.2 psu) was 22 km at 1200 m depth (see Figure 3). This isocontour is chosen with respect to the maximum salinity and temperature gradient for this deeper and larger core of the meddy.

In *Carton et al*. [2010], cyclone C1 was found northeast of M1. It was also shown that the interaction of M1 and C1 with another meddy and cyclone induced the coupling and eastward drift of M1-C1, as seen on RF1 trajectory (see Figure 4). After its eastward drift, float RF1 originally trapped in meddy M1 moved northward, then southward, and finally southeastward. Due to lack of in situ data at the time, *Carton et al*. [2010] used altimetric maps and a simple quasi-geostrophic model to show that this change of direction resulted a priori from the coupling of M1 with a cyclone other than C1.

3.2.2. Dipole Formed on Portimão Canyon in February 2001, M2-C2

MedTop hydrological sections, in February 2001, revealed the formation of a meddy coupled with a cyclone near Portimão Canyon, M2 and C2. Figure 5a shows the temperature and salinity distributions on the section from (36°14′N; 9°12′W) to (35°56′N; 8°14′W). In the northern part of this section lay meddy M2; this meddy occupied the 600–1500 m depth range. Its temperature maximum was 13.4°C near 900 m depth and its salinity reached 36.8 in a deep core between 1000 and 1400 m depths. Its radius, based on the 11.5°C isotherm, or on isohaline 36.2 psu, at 1200 m depth was about 25 km. The horizontal gradients of temperature and salinity at the periphery of meddy M2 were weaker toward northwest than southeast, where cyclone C2 lay.

Cyclone C2 had a temperature maximum equal to 11.4°C between 1100 and 1200 m depths; its salinity maximum, 36.4, was centered near 1200 m (see Figure 5a; Figure 5b provides another cross section of this cyclone). Furthermore, the spacing of isopynals (see Figure 6) became smaller between 1000 and 1400 m depth, characteristic of a cyclone; this was also confirmed by the calculation of the geostrophic velocity with a level of reference of no motion at 2000 m. Maximal velocities were on the order of -0.3 m s^{-1} for M2 and of 0.25 m s^{-1} for C2 and were found near 1200 m depth (see Figure 6). This figure also shows that:

1. The zero velocity line was tilted with respect to a vertical axis for both eddies; such a tilting is maybe achieved by the coupling between the two eddies in a stratified flow [*Dritschel*, 2002].

2. Both eddies had a surface signature in velocity, which was stronger above C2 than above M2; this intensification may be related to the existence of a separate structure above C2. The two velocity signals appear merged at 1200 m depth, but were separated by a third signal at the surface with an anticyclonic motion. This indicates that more dynamical structures (e.g., filaments) existed near the surface than at depth. Unfortunately, the map of Sea Level Anomaly for mid February 2001 (not shown) cannot evidence small-scale features at this location (due to the resolution of interpolated altimetric maps).

Considering the relative positions of M2 and C2, this dipole was moving southwestward at the time of its survey, in February 2001 (see Figure 7).

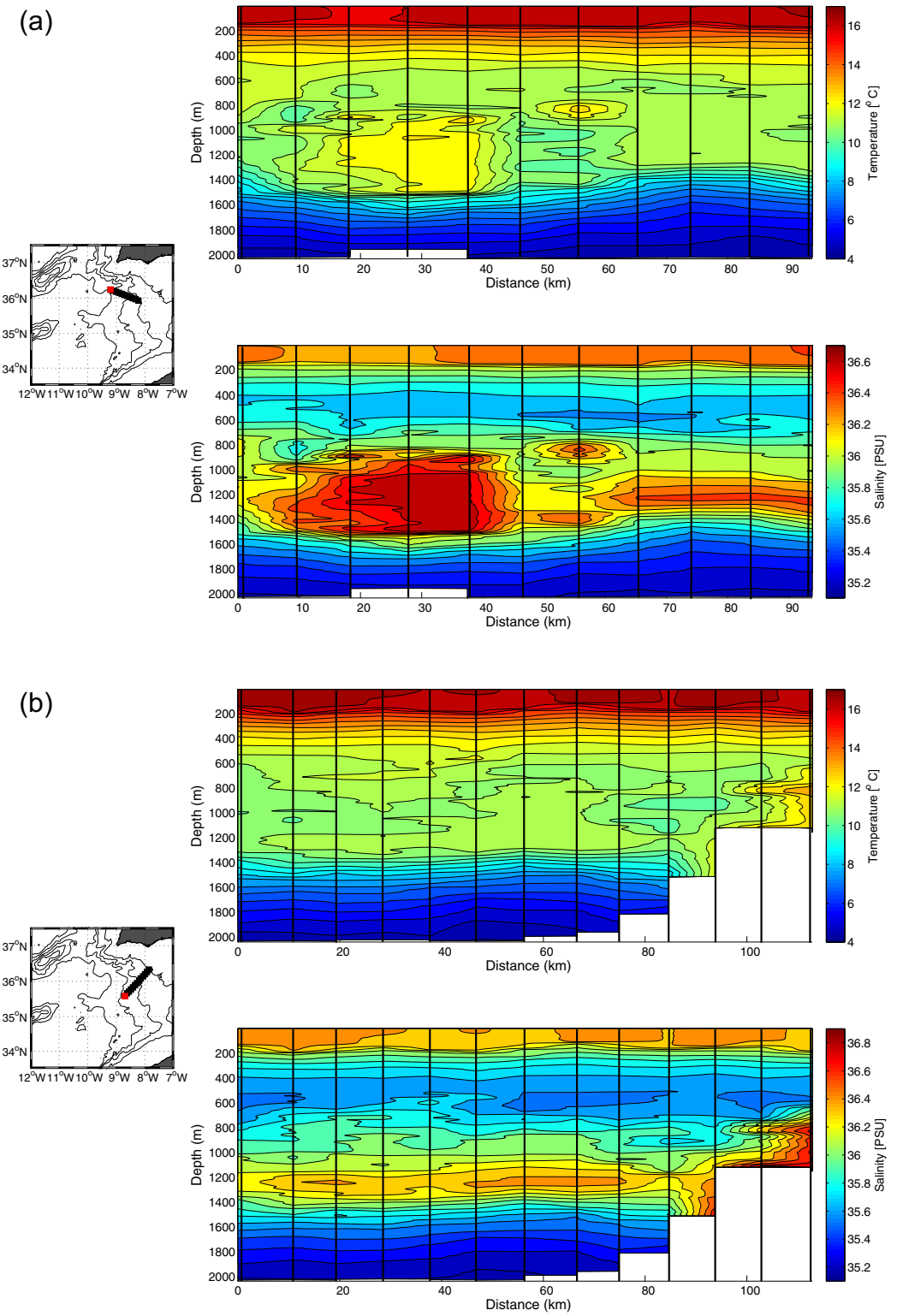

Figure 5. (a) Temperature and salinity distributions in (left) meddy M2 (between 5 and 45 km) and (right) cyclone C2 (from 60 km to the end of the section) on the transverse MedTop in February 2001 CTD cross section and (b) across the MW undercurrents on the (right) slope and (left) cyclone C2 (between 5 and 45 km). The distance is measured from the beginning of the section (red square). The anticyclone M2 has two cores, a first with a temperature maximum of 13.4°C near 900 m depth and a second with a salinity maximum of 36.8 psu between 1000 and 1400 m depths. The cyclone C2 has thermohaline maxima of 11.4°C and 36.4 psu near 1200 m depth.

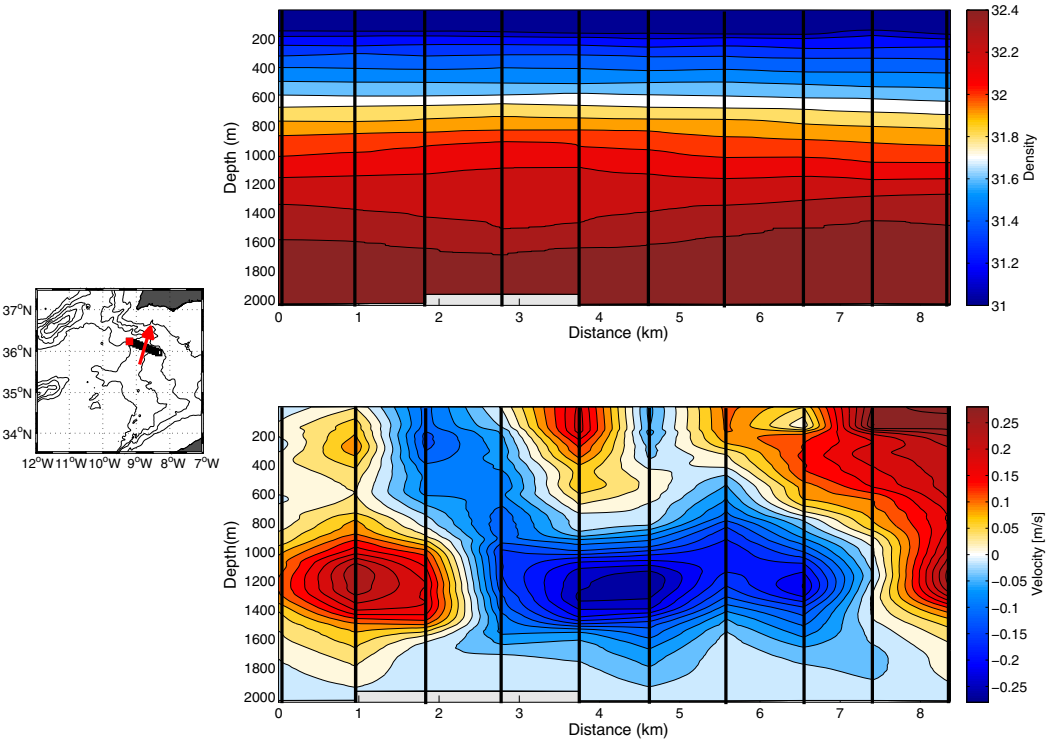

Figure 6. Potential density (σ_1, referenced at 1000 m) and geostrophic velocity distributions in (left) meddy M2 (between 5 and 45 km) and (right) cyclone C2 (between 50 and 85 km) with their centers around 1200 m, velocity is across the transverse MedTop cross section, the red arrow indicating the direction of positive velocity. Maximal velocities found near 1200 m depth with -0.3 m s^{-1} for M2 and 0.25 m s^{-1} for C2. Station positions are plotted as black vertical lines, the first position is pointed out by a red square on the map.

The M2-C2 dipole then collided with dipole M1-C1 as revealed by Rafos float RF2 trajectory (Figure 7a). Indeed, this trajectory was southwestward to 35°30′N, 10°W, a position close to that of M1 early April 2001. Thereafter, the loops performed by RF2 increased fourfold in radius and circled

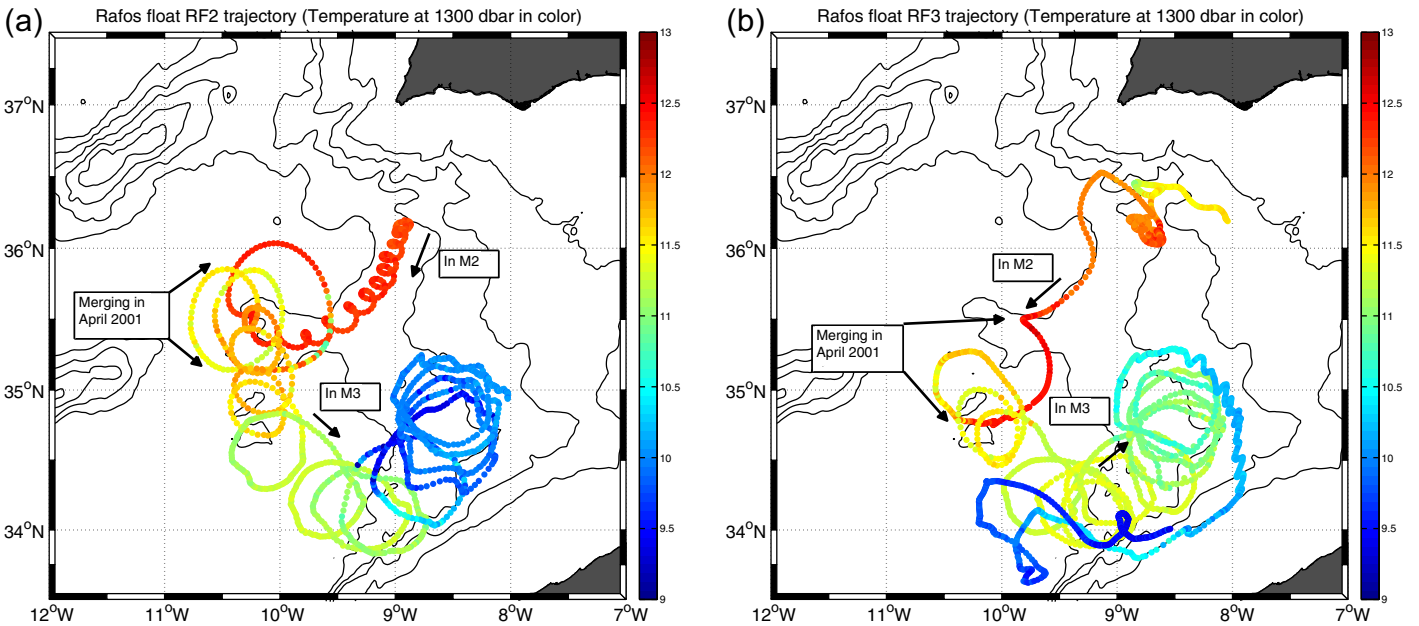

Figure 7. Trajectories of (a) Rafos float RF2 and (b) Rafos float RF3, of MedTop program, colored by temperature; they started respectively from about 36°15′N; 9°W and from 36°15′N; 8°W from February to September.

around the position of meddy M1 as shown by float RF1. This indicates that M2 strongly interacted with M1.

After this strong interaction, the trajectory of RF2 veered southward. The second part of this trajectory—between 35°30′N, 10°30′W and 34°N, 9°W seemed similar to that of RF1. To confirm this similarity, we separated the trajectories of floats RF1 and RF2 into mean drift and loops. The mean drift is represented in Figure 2c and was defined as the motion of the instantaneous center of rotation for each float. These were strikingly similar for both floats in this region. The center of rotation of RF2 was always less than 10 km away from that of RF1. Thus, the two floats must have drifted in the same meddy at that time. This meddy, M3, was the result of the interaction of M1 and M2.

We also show the trajectory of Rafos float RF3 (see Figure 7b). After its release east of Portimão Canyon, it followed the lower undercurrent of MW and drifted offshore along this canyon. It became trapped in an anticyclone (a meddy, near 36°15′N, 8°45′W) and was later ejected from this meddy to follow the continental slope. Again it veered offshore, from Cape Saint Vincent, and after two large anticyclonic loops, it reached the meddy containing RF1 and RF2, near 35°N, 10°W, in April 2001. This position also corresponded to the maximal temperature recorded by the float. From there on, its trajectory became comparable with that of RF2. The gradual decrease in temperature measured by the floats can be related to their progressive ejection from the meddy.

3.2.3. The Resulting Dipole in the Southern Gulf of Cadiz in July 2001, M3-C3

Figure 8 presents the zonal and meridional distributions of temperature and salinity of three selected XBT and XCTD sections, performed between 3 and 5 July, during Semane 2001 experiment. These sections were located between 34°N and 35°N meridionally, and 8°W and 10°W zonally.

On the quasi-meridional section (Figure 8a), one can identify a cyclone on the northern side and a meddy. The meddy position corresponds to the Rafos floats loops during this period. The cyclone is called C3 and the meddy M3 (labeled M6 in Figure 6 of *Serra et al.* [2010]). Now, we compare the hydrological properties of M3 with those of M1 and M2, and the characteristics of C3 with those of C2.

We recall that M1 and M2 had a 22 and 25 km radius, both based on isotherm 11.5°C, or isohaline 36.2 psu. Figure 8b indicates a radius of about 40 km for meddy M3, with the same isoline. Therefore, the salt and heat budgets advected in M1 and M2 cores, from isohaline 36.3 psu to focus on the cores of the meddies and to avoid diffusion, were, respectively, 3.4×10^{13} and 3.7×10^{13} kg of salt, and 4.5×10^{19} and 4.8×10^{19} J. The salt quantity calculated for M3 was 7.7×10^{13} kg and the heat was above 9×10^{19} J. The salt and heat from the inner cores of M1 and M2 almost equal those of M3, which indicates that an important mass transfer must have occurred from M2 to M1 to form M3. In terms of volume, M1 and M2 had vertical extensions of 800–900 and 650–700 m, respectively, and M3 about 950–1000 m. With respect to their radii, M3 had a more important volume (about 5×10^{12} m^3) than both M1 and M2 together (about 1.2×10^{12} and 1.4×10^{12} m^3), this could be due to entrainment of surrounding waters.

Figure 8b shows the salinity anomaly of M3 located between 600 and 1500 m depths, with a double core, similar to that of M1, and slightly more surface intensified than that of M2. On the Brunt-Väisälä frequency (not shown) two local minima were found between 500–800 and 1000–1500 m showing stability in those cores. This tendency was also found on M1 but M2 had only a local minimum between 1000 and 1500 m. The salinity peak of M3 (36.6 psu) was slightly below those of M1 and M2 (36.8 psu). The temperature of M3 reached 13.5°C and its anomaly was marked between 600 and 800 m depths, being closer to that of M1 than to that of M2.

Our interpretation is that during the merging process, meddy M2 wrapped around meddy M1, before their waters became mixed, transferring heat and salt to M1. The observed turbulent motions are likely to be related also to the kinetic energy and angular momentum redistributions caused by the meddy merger. During this merging, entrainment of surrounding North Atlantic Central Water (NACW) and eventually traces of North Atlantic Deep Water (NADW) led to a slight decrease in salinity.

Figure 9 shows the horizontal maps of temperature and salinity on three different isopycnals, obtained by optimal interpolation of the data over the 3 days of measurements, and using a 15 km radius of correlation; this radius corresponds to the average distance between two measurement points and the desired resolution but is smaller than that commonly used in the open ocean [*Arhan and Colin de Verdière*, 1985]. This is

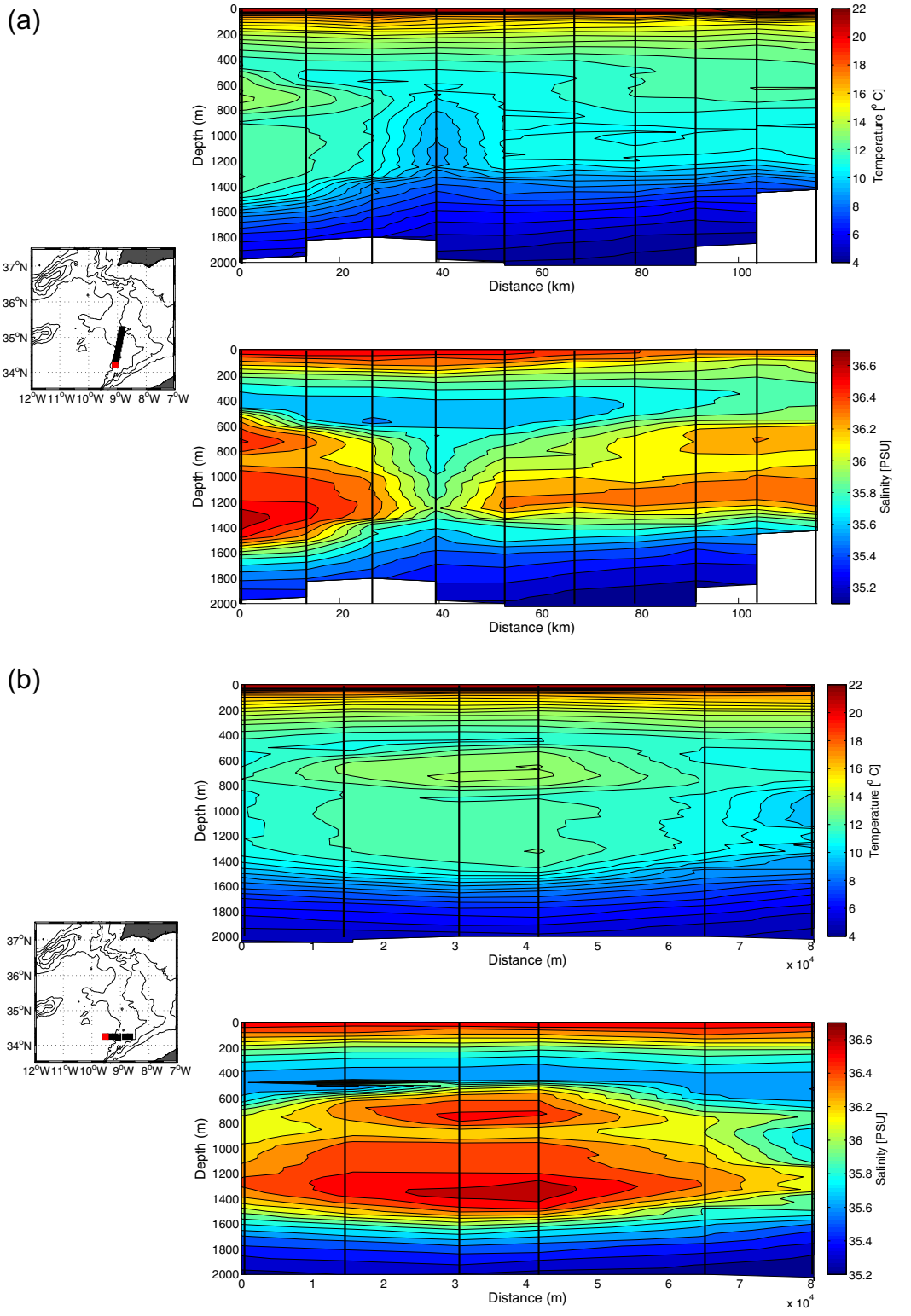

Figure 8. Meridional and zonal sections of temperature and salinity in the southern Gulf of Cadiz, during Semane 2001, in June 2001. (a) Quasi-meridional section across the meddy M3, between 0 and 35 km and cyclone C3, between 50 and 110 km; (b) zonal section of the meddy M3 at 34°20′N; (c) zonal section of the cyclone C3 at 35°N. The anticyclone has a salinity maximum of 36.6 psu between 1000 and 1500 m depths, the temperature maximum lies between 600 and 800 m depth with 13.5°C.

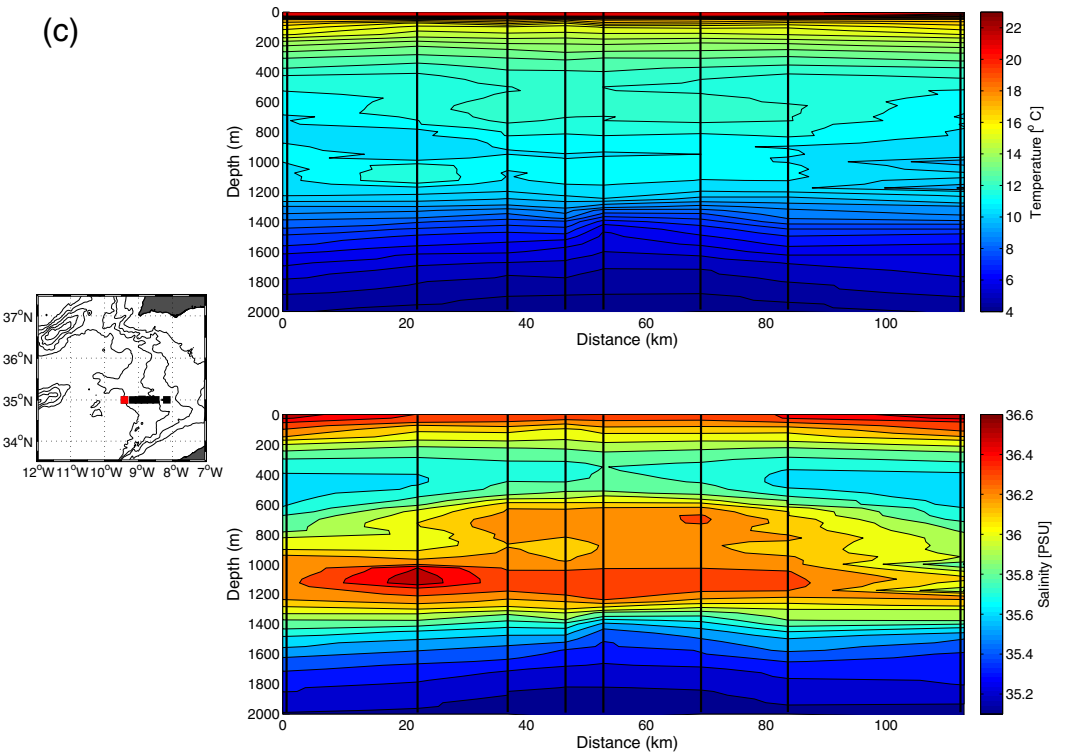

Figure 8. (continued)

also explained by the fact that we study mesoscale motions in a region with a moderately small deformation radius. At $\sigma_1 = 31.9$ kg m^{-3}, isopycnal with a mean depth of 800 m, the warm waters of the cyclone (north) and meddy (south), with temperatures on the order of 12–12.5°C were separated by a strip of colder water (on the order of 10°C); this strip was about 30 km wide meridionally. The salinity distribution displayed a similar pattern, with two peaks at 36.2 and 36.4 psu (for the meddy and cyclone) separated by a strip of freshwater (with salinity 35.6–35.7 psu). This water is NACW. Supposedly, this strip has been advected eastward by the joint rotation of the meddy and cyclone; it has been elongated by the strain field created by the two eddies. This situation is reminiscent of that observed during Semane 99 [*Carton et al.*, 2002] but here without an external source of Mediterranean Water.

The isopycnal $\sigma_1 = 32$ kg m^{-3}, having a mean depth of 1000 m, is situated between the two cores of the eddies, resulting in lower values of temperature and salinity for the meddy and the cyclone (12.5°C and 36.5 psu for the meddy versus 11.5°C and 36.2 psu for the cyclone). At $\sigma_1 = 32.2$ kg m^{-3}, isopycnal with a mean depth of 1200 m, the temperature of the meddy was much higher than that of the cyclone (12°C versus 10.5–11°C). This could be due to the entrainment of NADW below the cyclone core during its formation, and to its mixing with Mediterranean Water. Finally, for the same isopycnal, the water tongue between the two eddies may have resulted from a turbulent horizontal diffusion of salt due to the strong interaction between these eddies.

The geostrophic velocity maximum calculated in M3 (not shown), with a level of no motion at 2000 m, was about 0.25 m s^{-1} at 750 m depth and at a radius of about 10 km from the meddy center. The velocity was still 0.15 m s^{-1} at 1000 m depth. These values were slightly below the velocities recorded by the float (about 0.2 m s^{-1}). The M1 and M2 velocities were, respectively, 0.3 and 0.5 m s^{-1}. Therefore, both the interaction and propagation off the eddies have affected their kinetic energies. With respect to their volume, the sum of M1 and M2 kinetic energies (about 6×10^{10} J) was more important than the M3 kinetic energy (about 3.8×10^{10} J), here again it could be due to entrainment of surrounding waters around M3, and/or to the loss of M1 or M2 fluid to the environment. Kinetic energy variation after eddy merger has been discussed in theoretical studies (see below, the modeling part).

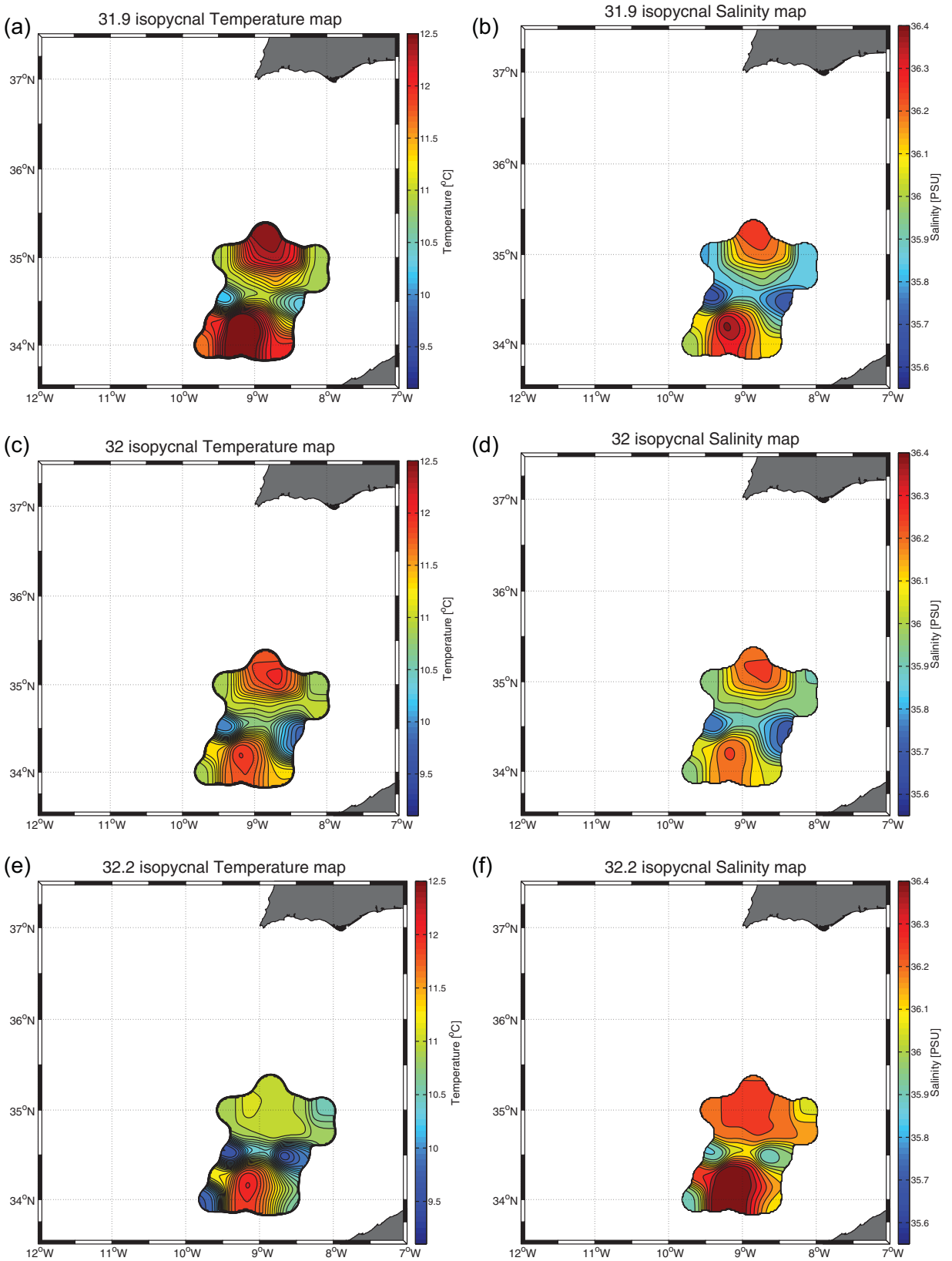

Figure 9. Horizontal maps of (left) temperature and (right) salinity in the southern Gulf of Cadiz, during Semane 2001, in June 2001. (top) At $\sigma_1 = 31.9$ kg m^{-3}, the upper core of M3 (south) and the core of C3 (north) show strong thermohaline anomalies, separated by a strip of fresher and colder water. (middle) On isopycnal $\sigma_1 = 32$ kg m^{-3}, out of the eddy cores, temperature, and salinity anomalies decrease. (bottom) On $\sigma_1 = 32.2$ kg m^{-3}, higher temperature is observed in M3 than in C3, due to turbulent diffusion of NACW and MW.

3.3. Detailed Analysis of the Eddy Interaction, From Float Trajectories and Altimetric Data

To understand more precisely the interaction between M1 and M2 (with the influence of C1 and C2), we segmented in Figure 10 the trajectories of floats RF1, RF2, and RF3, in monthly periods from March to August. In July and August, float RF1 is substituted by float SF released in M3. We recall that SF is a Surdrift buoy launched in M3 in June 2001. We superimposed these segments on the SLA map corresponding to the middle of each period. We named the main features SA and SC for surface anticyclone and surface cyclone. We also compared the trajectories of the floats with SST anomaly that is the difference between a monthly averaged map of SST and 23 year climatological months. We repeated the positions and names of the main features detected on altimetry on these SST anomaly maps. The joint use of SLA and SST anomalies gave us an indication of mid depth structures [*Bashmachnikov et al*., 2013]. Positive SLA and SST anomalies show that an anticyclone is located near the surface. Negative anomalies for both altimetry and SST correspond to a cyclone. Positive SLA anomaly with a negative SST anomaly corresponds to an eddy that lies at depth, e.g., a meddy.

On the first map (March 2001, Figure 10a), all floats were clearly separated. RF1, released in M1 was looping anticyclonically under a patch of positive SLA (SA2 on the maps) near 36°N, 10°W; RF2, released in M2 was rotating anticyclonically with small loops (20 km in diameter) while following a clockwise trajectory around the aforementioned positive SLA. RF3 was moving almost zonally on the southern side of the Iberian peninsula coast but it headed southward along 8°45′W and started looping anticyclonically (with small loops, of 15 km diameter) under a negative patch of SLA, which could be continuously tracked until the Semane 2001 survey in July. We call SC2 the cyclone corresponding to this negative SLA. Furthermore, at that time, RF3 was quite far (by about 80 km) from the two other floats. This may indicate that it was trapped in a small anticyclonic eddy of MW formed after M2 or as a spin-off of M2 formation. In Figure 11a, the corresponding SST anomaly field showed a negative anomaly advected southward, at the position of SC2 (36°N and 9°30′W). This can be the signature of a subsurface cyclone, C3.

In April, the correlation between trajectories and altimetry becomes clearer (see Figure 10b), we observe here the merger. RF1 and RF2 loops became much larger (80 km in diameter, suggesting a merger of M1 and M2). Both floats rotated anticyclonically under a positive SLA patch (SA2) extending from 35°N to 37°N along 10°30′W. This positive SLA matched in position to a strongly SST negative anomaly corresponding to a meddy (Figure 11b). A substantial amount of fluid must have been transferred from M2 onto M1 at that time explaining the exchange of float RF2 between the two meddies and leading to the final meddy M3. This negative SST anomaly patch also extends toward the altimetric signature of C3, suggesting that M3 was elongated due to shear created by the neighboring cyclone (C3). At the same time, float RF3 circled cyclonically around SC2 near 36°30′N, 9°30′W. The trajectory of this float also displayed two anticyclonic meanders a priori influenced by meddy M3.

In May, all three floats started drifting in M3 whose altimetric signature gradually decreased in amplitude, while the altimetric signature of the accompanying cyclone (C3) remained strong. The SST negative anomaly from both SC2 and SA2 intensified. The diameter of the RF2 loops decreased from April to May, showing an adjustment of M3 after the merger of M1 and M2. The temperature measured by RF2 also dropped by 1°C at that time (see Figure 7a). This can be explained as follows: the M1 and M2 interaction increased the thermohaline gradients of M3; thus, any radial shift of float trajectory in the meddy may have led to a noticeable increase or decrease in the measured temperature.

In June 2001, the loops in the trajectories of the three floats became elongated; as the meddy M3 became deformed elliptically. This deformation is coherent with an anticlockwise acceleration of M3 around C3 at that time. Float RF2 recorded a lower temperature as it moved outward in the meddy, starting in early July 2001.

These float trajectories show that M3 was following a cyclonic trajectory in the Gulf of Cadiz, a priori under the influence of the neighboring vortices (and in particular of C3), but this trajectory was also in agreement with the regional circulation. The SST anomalies map of June (Figure 11d) also showed a cyclonic motion of the warmer water near M3 and around C3.

During Semane 2001, several deep-drogued Surdrift buoys were used. Here, we study in particular SF which was released on 5 July 2001 at 34°12′N, 9°05′W, and had a drogue at 1050 m depth. This buoy performed several loops in M3 and drifted in a northeastward direction before turning back southwestward along the Moroccan coast.

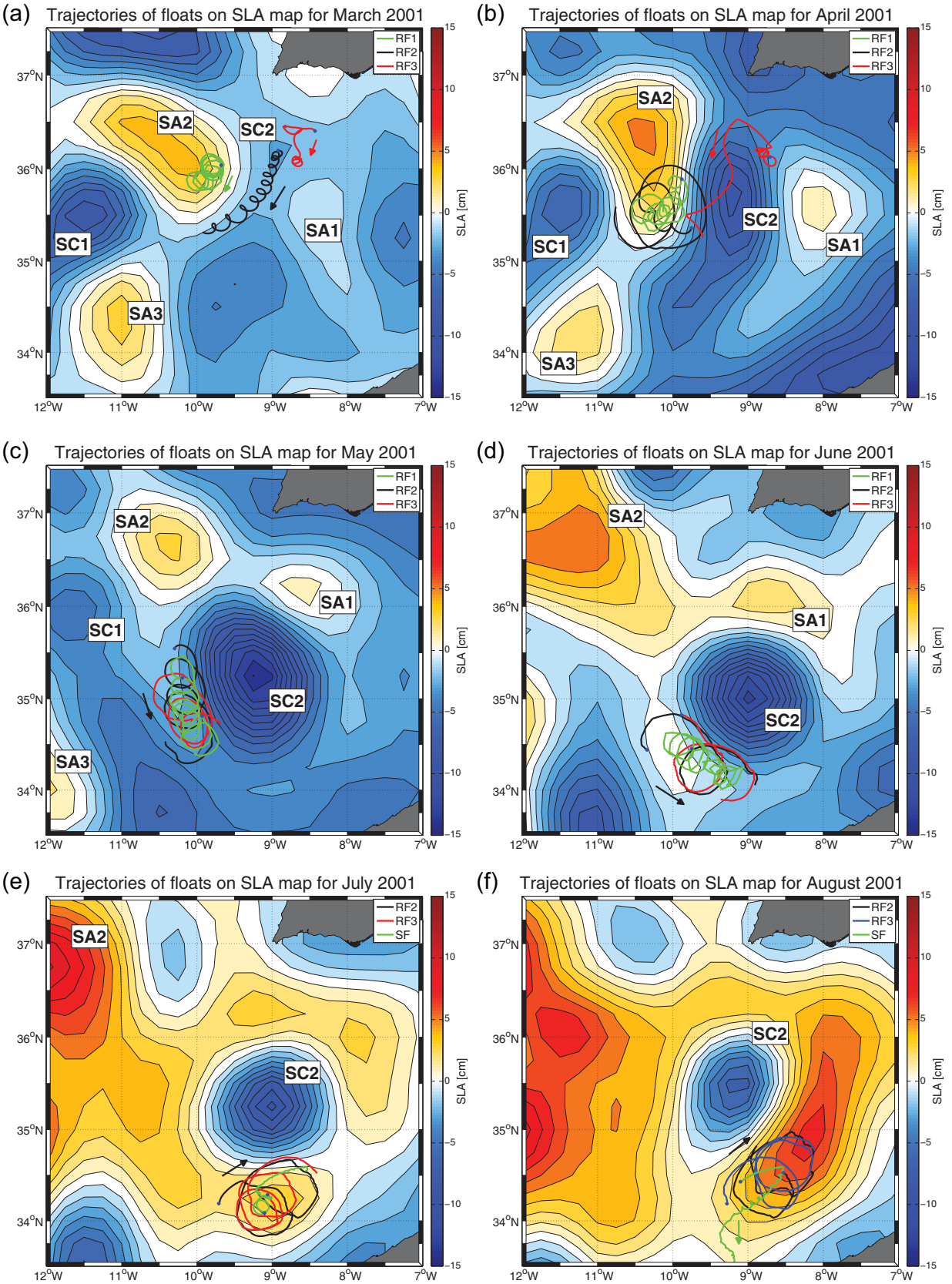

Figure 10. Superposition of trajectories of Rafos floats RF1 (green), RF2 (black), and RF3 (red, except blue on the last map) on altimetric maps (Sea Level Anomaly in cm); from left to right and from top to bottom, months are March to August 2001. For July and August, the green trajectory corresponds to buoy SF.

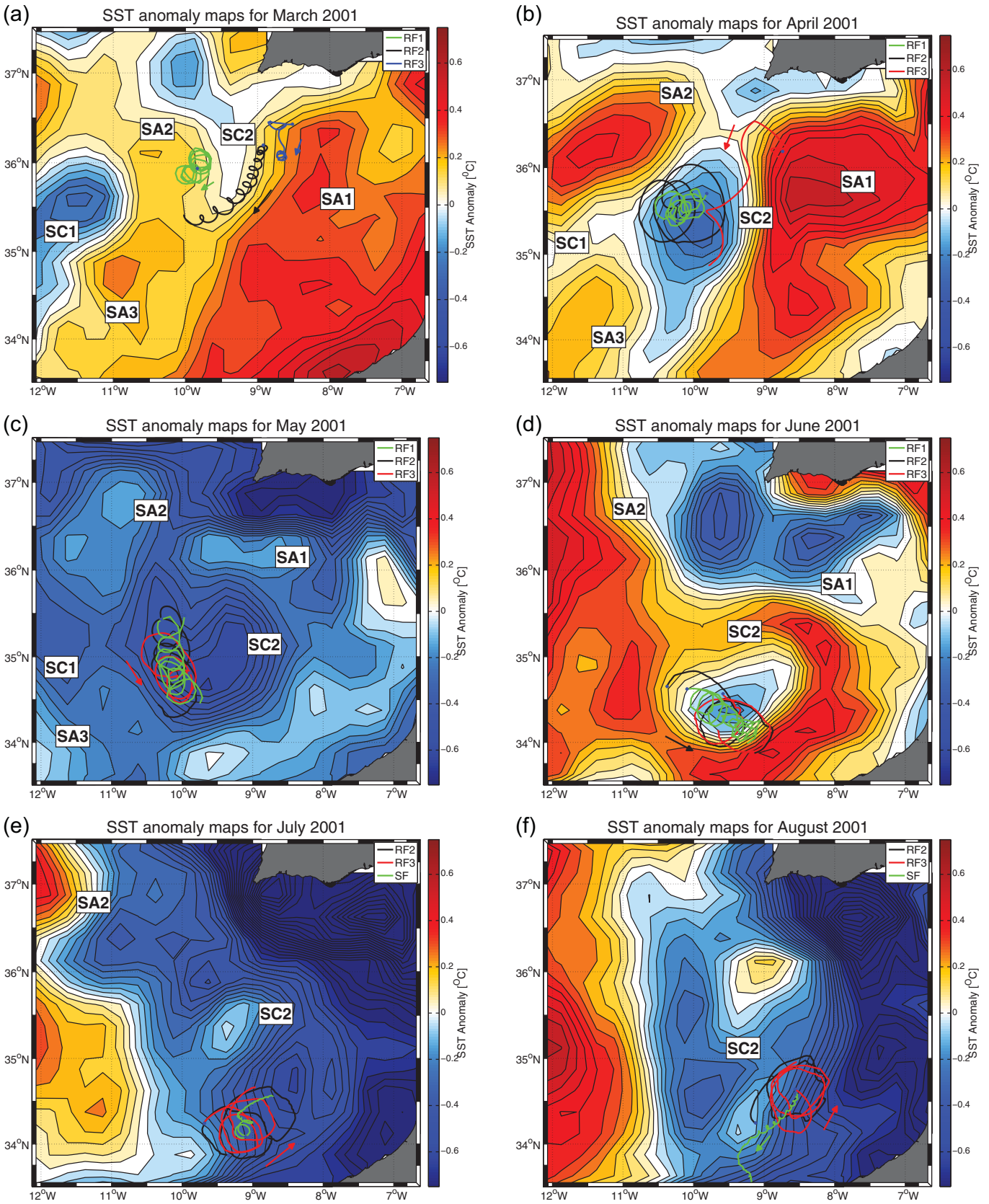

Figure 11. Monthly averaged Sea Surface Temperature anomalies maps corresponding to the Figure 10, months are March 2001 to August 2001, with superimposition of floats trajectories.

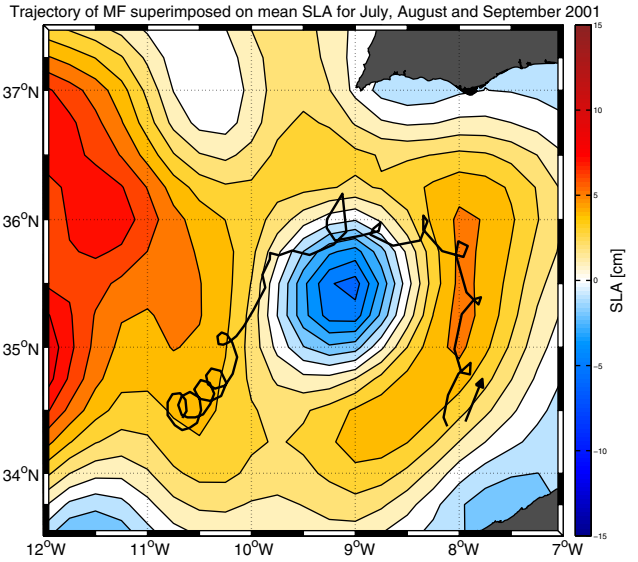

Figure 12. Trajectory of a MARVOR (multicycle acoustic float) drifting at 450 dbar, from end of June until end of September 2001 superimposed on SLA. The float rotates around a strong negative altimetric anomaly all along its trajectory while spinning in anticyclonic loops. It suggests that the float is following a meddy rotating around a strong cyclone.

In July, all floats and buoys were looping in M3, which was heading northeastward (see Figure 10e). In August, the surface signature of M3 intensified while this meddy was still rotating around C3. This signature became also strongly elongated at that time, as if M3 was joining another eddy; the SST anomalies map (Figure 11f) showed a propagation of warm water near 36°N–8°30′W). However, the trajectories of Rafos floats RF2 and RF3 do not show any sign of elongation [*Lamb*, 1993]. Note that the drogue of buoy SF broke around that time, and that the buoy then performed small inertial loops while drifting southwestward. A multicycle acoustically tracked float from the ARCANE experiment, drifting at 450 dbar, performed anticyclonic loops and drifted anticlockwise in the Gulf of Cadiz during July, August, and September 2001 around C3. Its trajectory is shown in Figure 12. We are primarily interested in the segment of trajectory in July 2001. There is a clear correspondence between the float position on July and the SLA map with a positive patch near 36°N, 8°W. Thus, there was another anticyclone (SA4, not shown on the map), perhaps a meddy, in the eastern Gulf of Cadiz during the same lapse of time. Finally, at the end of August, buoy SF was ejected from M3 while RF2 and RF3 were still regularly rotating in this eddy, without any influence of a meddy to its north. During July and August, the surface signature of C3 barely evolved.

4. Numerical Modeling of the MW Dipole Collision

4.1. The Model

We used a three-layer quasi-geostrophic model to investigate the mechanism of interaction between dipoles M1-C1 and M2-C2. Since this interaction took place far from the continents and high above the bottom, we used a flat-bottom, open-ocean model. More specifically, the model domain is square and horizontally biperiodic, but the eddy interaction takes place near the center of the domain so that periodicity influences are negligible. A beta-plane configuration was implemented.

We chose a length scale L = 40 km and a velocity scale $V_0 = 1$ m s^{-1}. Our dimensionless domain length was 4π or in dimensional terms 502 km. This is about 4.5° of latitude and 5.5° of longitude. The resolution was 256 × 256 points (one point every 2 km).

The quasi-geostrophic equations for potential vorticity are in layerwise form:

$$\frac{dq_j}{dt} = \nu_2\nabla^4\psi_j + \nu_4\nabla^6\psi_j$$

where $\psi_j(x, y, t)$ is the stream function and q_j is the potential vorticity in layer j

$$q_j = \nabla^2\psi_j + F_{j,j-1}(\psi_{j-1} - \psi_j) + F_{j,j+1}(\psi_{j+1} - \psi_j) + f_0 + \beta y$$

where applicable (i.e., there is no coupling of the upper layer with the atmosphere, nor of the lower layer with the bottom). The coupling coefficients are

$$F_{j,j-1}=f_0^2/(g'_{j-1/2}H_j), \quad g'_{j-1/2}=g(\rho_j-\rho_{j-1})/\rho_0$$

where $f_0 = 8.34 \times 10^{-5}$ s^{-1} is the Coriolis parameter at 35°N, H_j is the thickness of layer j ($H_1 = 600$ m, $H_2 = 900$ m, $H_3 = 2500$ m). The beta value is $\beta = 1.86 \times 10^{-11}$ m^{-1} s^{-1}. All these parameters are made dimensionless in the model.

The stratification of this model is fitted to the region: the reduced gravities $g'_{j-1/2}$ are calculated such that the external deformation radius is infinite and the first two internal deformation radii are 30 and 15 km, respectively [see *Carton et al*., 2014]. We have $\frac{\Delta\rho_1}{\rho_0} = 10^{-3}$ and $\frac{\Delta\rho_2}{\rho_0} = 3\times10^{-4}$.

The model performs spatial derivatives via a Galerkin projection on Fourier modes with truncation and a mixed Euler-leapfrog time stepping scheme is used.

The vorticity dissipation in the model is achieved with a harmonic and a biharmonic operator; the two viscosities are maintained to a minimum compatible with the absence of noise at small scales. The dimensional values are $\nu_2 = 0.4$ m^2 s^{-1} and $\nu_4 = 3.2\ 10^7$ m^4 s^{-1}, which are very low.

For simplicity, we confined the eddy velocity in the middle layer (note that potential vorticity thus exists in all layers):

$$V_1=V_3=0, \quad V_2=V_0(r/R)exp(-r^2/R^2), \quad r^2=(x-x_0)^2+(y-y_0)^2$$

where x_0 and y_0 are the coordinates of the eddy center. The Gaussian velocity profile is commonly used for MW eddies [see *Carton et al*., 2014]. Therefore, each eddy is characterized by four parameters V_0, R, x_0, y_0. Note that the velocity maximum is $V_{max} = V_0/\sqrt{2e}$ at a radius $R_{max} = R/\sqrt{2}$.

4.2. The Numerical Experiment Simulating the Observations

To reproduce the details of the interaction between the two dipoles, we started from the February 2001 situation. The previous stage of the evolution of M1-C1 has indeed been modeled before. This date corresponds to the formation of M2-C2 south of Portimão Canyon and thus to detailed measurements of this dipole. We do not have hydrological measurements of M1-C1 at the same date but we can estimate that its structure has not changed much since November 2000, but for a slight attenuation.

Also we center this situation in the middle of our domain, so that the origin is now at 36°N, 9°W. We locate M1-C1 using the Rafos floats trapped in M1, and we use the trajectory of M1 center (southward at that time) to infer that C1 lay east of M1 at that time (see Figures 2a and 2b). The velocity of C1 is that used in *Carton et al*. [2010]. The velocity of M1 was chosen equal to 80% of its value in November 2000 to allow for a slight decay since its first observation.

Therefore, the parameters for this situation are, in dimensionless form:

Note that, for instance, $V_0 = 0.93$ corresponds to $V_{max} = 0.4$ m s^{-1} (and $V_0 = 0.7$–0.3 m s^{-1}); $R = 0.707$ leads to $R_{max} = 20$ km (Table 2).

In Figure 13, horizontal maps of potential vorticity in the middle layer are shown, zoomed in on the central region where interaction occurs (that is, in a 251 × 251 km). The initial position of M2-C2 is near Portimão Canyon, shifted here to the northeastern part of the subdomain. The initial position of M1-C1 is about 100 km further west and about 15 km north of the latter. Initially, C1 is east of M1 and C2 is southeast of M2. This corresponds to the February situation.

Table 2. Table of the Numerical Experiment Parameters

Eddy	V_0	R	x_0	y_0
M1	−0.93	0.353	−2.2	0.6
C1	0.93	0.53	−1.5	0.6
M2	−0.7	0.53	0.3	0.6
C2	0.7	0.53	1.2	0.0

After 2 weeks, dipole M1-C1 has rotated cyclonically (C1 having a larger circulation than M1) and dipole M2-C2 has propagated southwestward. After 3 weeks, M2 is advected by C1, C2, and M2 and deformed by the flow field of these three eddies. M2 is considerably elongated. After 4 weeks, the merger of M1 and M2 takes place. A substantial mass transfer occurs from M2 to M1; but as it

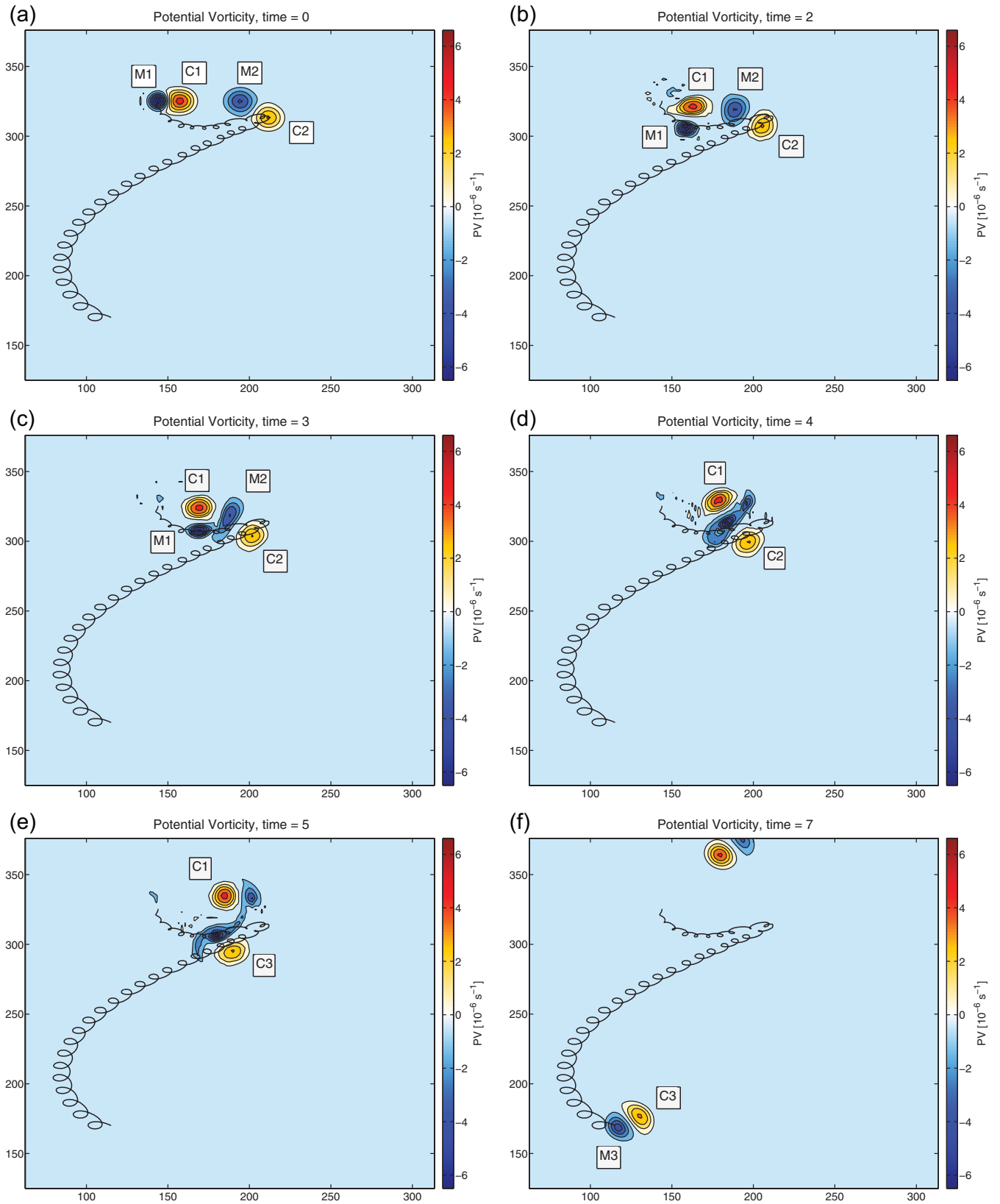

Figure 13. Time series of potential vorticity maps in the middle layer (zoomed in on km 125–375 zonally and on km 62–312 meridionally); PV contour interval is $110^{-6}s^{-1}$; times shown are 0, 2, 3, 4, 5, and 20 weeks of simulation; with superimposition of the trajectory of a Lagrangian float launched in the western meddy. The change of the cyclone name "C2" to "C3" from plots 4 to 5 is to fit with the section 3.

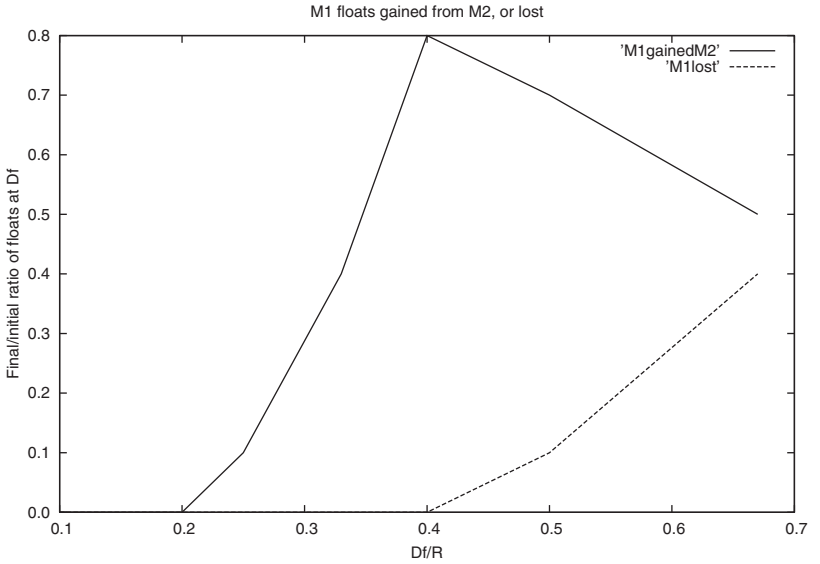

Figure 14. Ratio of the floats initially in M2 and finally found in M1 ("M1gainedM2"), and of floats initially in M1 lost to the surrounding flow ("M1lost") with respect to the distances D_f to the meddy center.

is frequent with asymmetric merger, a fragment of M2 is shed during the process (in the observations, it seems that all of M2 merged with M1). After 5 weeks, the two meddies have separated and about 30% of M2 has remained coupled with C1. This asymmetric dipole will rotate cyclonically over a short distance in the northern part of the domain as can be seen on potential vorticity plots of weeks 7 and 20. Thus, there has been an exchange of cyclones between the two meddies. On the same plots, it can be seen that C2 and what is now called M3, drift first southwestward and then southeastward, also cyclonically, as in the observations. This suggests that C3 is C2.

The efficiency of this merger process between M1 and M2 is now quantified with two diagnostics.

First, we seeded artificial floats in each meddy, at the initial stage of the simulation. These floats were seeded by groups of 10, regularly spaced azimuthally, and at different distances D_f from each meddy center. We let D_f range from 0.1 to 0.7 meddy radii. In Figure 14, we show how many floats initially in M2 were finally found in M1 ("M1gainedM2") and how many floats initially in M1 were lost to the surrounding flow ("M1lost"). This figure shows that floats were torn from deep in the M2 core (10% of the flows at $D_f = 0.25R$ were finally found in M1). This figure increases to 80% for $D_f = 0.4R$ and it decreases to 50% for $D_f = 0.67R$. This is simply explained by the fact that peripheral floats can be expelled from M2 into the surrounding ocean (e.g., in filaments) and not be absorbed by M1. The second curve shows that M1 itself lost its peripheral floats during the merging process.

In short, M2 was severely disrupted by the merging process (as far inward as a quarter of its radius) and lost much of its mass essentially to M1 but also to the surrounding ocean. This is compatible with the fact that only a minor fraction of M2 finally drifted with C1. During merger, M1 also lost a part of its external envelope.

The second diagnostics that we performed was the computation of the area integral of potential vorticity for M1 in its main (intermediate) layer. We found that M1 gained 50% of surface integrated potential vorticity. Again, such a value is compatible with the final remainder of M2. This value can be also used as an estimate for the change in tracer contents (e.g., salt contents). Theoretical studies [e.g., *Cushman Roisin*, 1989] have detailed the conditions under which the conservation of local or integral invariants is possible during eddy merger. In particular, the conservation of both potential vorticity, angular momentum, mass and kinetic energy, was shown possible only if filaments were formed at the end of the merging process. These filaments (modeled as a vorticity ring in the theory) would carry only a minor fraction of mass or of kinetic energy but the vast majority of angular momentum. This has two implications: first, these filaments are usually thin and are more sensitive to dissipation so that part of the initial kinetic energy can be lost after merger; second, as stated in *Cushman Roisin* [1989], the process of eddy growth and of filament formation

Table 3. Table of the Numerical Experiment Parameters for Collinear, Opposite, and Symmetric Dipoles

Eddy	V_0	R	x_0	y_0
A1	−0.7	0.53	−1.5	−0.4
C1	0.7	0.53	−1.5	0.4
A2	−0.7	0.53	1.5	0.4 offset
C2	0.7	0.53	1.5	−0.4 offset

is the physical manifestation of the inverse energy and direct enstrophy cascades, typical of quasi-2-D turbulence.

4.3. Sensitivity Tests and Constraints for the Realization of the Observed Phenomenon

It must be noted that this evolution also occurred for other initial conditions. First, if the eddies had slightly different velocities or positions, partial merger of M1 and M2 was also observed. But the efficiency of the merger process was weaker in the other experiments we performed. Also, the final trajectory of the stronger dipole was more often southwestward.

Second, even if M1-C1 drifted eastward from an initial western position, merger of M1 with M2 could be obtained with a further cyclonic trajectory of the resulting dipole (southwestward, then southeastward; plots not shown here). Thus, this evolution is not unique.

Therefore, we search the conditions under which this merger and/or the exchange of cyclonic companion can occur. To this aim, many numerical simulations were conducted.

As a preliminary note, we can recall that it is impossible to forecast exactly the evolution of the four vortex system due to the irreversible processes which occur during the interaction (vortex deformation, filamentation, merger, or splitting). This interaction is not comparable with that of four point vortices, except if they are widely separated (furthermore, the evolution of four point vortices is most often chaotic).

4.3.1. Collision of Collinear, Opposite, Symmetric Dipoles

To assess how the offset collision of dipoles can result in the merger of two of their eddies, we first analyzed the collision of two equal, symmetric dipoles on the beta plane. These dipoles were propagating in opposite directions (one eastward, the other one westward). We varied the offset between their (zonal) propagation axes (see Table 3). Hereafter, we call A the anticyclones and C the cyclones, which may not have the characteristics of the meddies nor of the MW cyclones.

Whatever the case (head-on or offset collision), no merger occurred between the anticyclones, even if they partially interacted for a short time. This temporary interaction and exchange of fluid is in agreement with the study by *Velasco Fuentes and Van Heijst* [1995]. Here, we observed that the cyclones simply exchanged partners and finally rotated to adopt an eastward propagation on the beta plane (the stationary configuration) [see *Velasco Fuentes and Van Heijst*, 1995]. Changing the intensity or size of the eddies (to 0.5 or to 0.7) did not change this evolution qualitatively.

4.3.2. Collision of Opposite, Symmetric Dipoles With a Finite Angle Between Orientations

Starting from this observation, we studied the collision of the same symmetric dipoles, but now propagating southeastward and southwestward, respectively (Table 4). This initial orientation should favor the merger of the anticyclones, provided that they are located at the proper initial position.

For A1-C1, we chose an initial position symmetric of that of M2-C2 in the observations. For A2-C2, we allowed a variation in latitude to create an offset in the collision. These initial positions were calculated with the help of a point vortex model to obtain a first guess of the dipole trajectories.

Only when the two anticyclones came close to each other in the collision, did they merge (for an offset of about 0.6); under other circumstances, the shear and strain created by the neighboring cyclones was sufficient to pull the anticyclones apart. The most efficient merger occurred if A2 passed 5 km south of A1 (offset of 0.7). In that case, the merger efficiency was about 90%. This efficiency decreased to 50% if the anticyclones drifted 10 km apart (offset of 0.8).

Table 4. Table of the Numerical Experiment Parameters for Opposite, Symmetric Dipoles With a Finite Angle Between Orientations

Eddy	V_0	R	x_0	y_0
A1	−1.0	0.53	−2.0	0.8
C1	1.0	0.53	−1.4	1.4
A2	−1.0	0.53	1.4	1.4-offset
C2	1.0	0.53	2.0	0.8-offset

4.3.3. Collision of Opposite, Asymmetric Dipoles

Finally, we studied the collision of two opposite, asymmetric dipoles. The ratio of stronger to weaker eddy velocity in each dipole was 0.6 (the dipoles were initially NW and NE of the domain; see Table 5). To find the

Table 5. Table of the Numerical Experiment Parameters for Opposite, Asymmetric Dipoles

Eddy	V_0	R	x_0	y_0
A1	−0.6	0.53	−2.0	0.8
C1	1.0	0.53	−1.4	1.4
A2	−1.0	0.53	1.4	1.4 offset
C2	0.6	0.53	2.0	0.8 offset

initial position of the dipoles, a four point vortex model was used, with equivalent circulations. Though this point vortex model was on the f-plane, it provided a fair estimate of the initial trajectory of the dipoles (before they interacted). This way, we could control the offset of the dipoles when they collided.

In this case, strong interaction between the anticyclones took place when they collided head-on (offset of about 0.6). But since C1 was stronger than C2, it paired with the strongest anticyclone resulting from the interaction. Only the weakest anticyclone drifted southwestward with C2. Again the most efficient merger occurred if A2 passed 5 km south of A1. In that case, the merger efficiency was about 40%.

4.4. Conclusions of the Modeling Part

This very simple modeling of the collision between two dipoles on the beta plane has shown that the observed situation could be reproduced with few parameters (eddy radii, intensities, positions) for the model and a simplified structure (Gaussian distribution of stream function) for the eddies. Setting the eddy parameters on the available observations, the observed meddy merger and further trajectory could be reproduced fairly well; in the model, meddy merger was not complete, contrary to observations, but the strength of all eddies involved was not exactly known at the time; this may account for this difference. Several diagnostics were implemented on this simulation, indicating that M2 was strongly eroded during the merging process. A substantial part of its mass was absorbed by M1 (as shown by the float count and by the integral budget of potential vorticity). Other experiments showed that meddy merger and southward drift also occurred when the eddy parameters were slightly changed or if M1-C1 came from the west instead of the north.

A series of idealized experiments, designed to test the conditions under which this evolution could take place, provided the following results:

1. the head-on or offset collision of collinear symmetric dipoles cannot lead to the same evolution because of the shear created by the cyclones on the anticyclones; this shear separates the anticyclones after they start merging; this is in agreement with a previous study by *Velasco Fuentes and Van Heijst* [1995];

2. the head-on or offset collision of asymmetric dipoles coming from the NW and from the NE can lead to anticyclone merger but the stronger resulting anticyclone then moves eastward with the stronger cyclone;

3. the lateral collision (at a finite angle) of such dipoles can lead to a merger of the anticyclones if these latter collide nearly head-on, but again this merger is not complete.

Thus, the complete merger of M1 and M2 was certainly due to their position during the collision (only slightly shifted) and to the fact that the accompanying cyclones were not strong enough to tear apart the resulting meddy, but sufficiently strong (and comparable in strengths) to advect it anticlockwise after the merger.

5. Conclusion and Discussion

A unique joint data set has allowed the characterization of two dipoles of Mediterranean Water in the Gulf of Cadiz. The western dipole (M1 and C1) could not be completely described by lack of hydrological data, but its meddy was fully studied in *Carton et al*. [2010]. The Portimão dipole (M2 and C2), which had been described previously in *Serra et al*. [2005], *Ambar et al*. [2008], and *Serra et al*. [2010], has been identified as the structure colliding with the western dipole, in the present paper.

The western dipole drifted northeastward from its position southwest of Cape Saint Vincent, while the Portimão dipole drifted southwestward from the Canyon. They collided near 35°30′N, 10°W. In this process, the two meddies merged while the cyclones drifted apart. More precisely, M2 wrapped around M1 before merging with it and forming M3. M3 then drifted southeastward, coupled with a cyclone that we called C3. It should be noted that only a few complete observations of oceanic eddy merger are reported in the literature [*Creswell*, 1982; *Schultz-Tokos et al*., 1994; *Richardson et al*., 2000]. They showed mass

transfer between meddies. This collision is original because it presented the interaction of two dipoles, instead of meddies.

Eddies M3 and C3 were finally surveyed in early July 2001 in the southern Gulf of Cadiz during a Semane experiment. These hydrological sections confirmed that cyclone C3 was in fact C2 and that M3 was much larger than M2 or M1, thus supporting the hypothesis of a large mass transfer between M2 and M1. The similarity of the thermohaline characteristics also supported our description of the dipole interaction.

In fact, the hydrological and dynamical situation in the Gulf of Cadiz in April 2001 to June 2001 was more complex than the interaction of two dipoles of MW: surface maps and float trajectories point toward a very complex mesoscale field, a priori with many meddies and cyclones in the Gulf of Cadiz (as suggested by the altimetric maps of Figure 10). The general motion of these meddies and cyclones was anticlockwise east of 11°W.

More generally, this shows that meddy collisions/mergers are likely to occur close to sites of meddy (and MW cyclone) generation. The meddy-cyclone coupling, often observed recently, leads to a faster propagation velocity than that of the beta-drift of a meddy, and also to more energetic and more complex collisions (larger "efficient section"). As such, these dipoles collisions, at the MW level, may be an efficient mechanism to generate the larger meddies that are encountered further outside of the Gulf of Cadiz [e.g., *Armi and Zenk*, 1984]. This would make the Gulf of Cadiz a "cauldron," somehow alike to the "Cape Cauldron" [*Boebel et al*., 2003]. These strong nonlinear interactions may also trigger spiral arms recently observed around meddies [*Song et al*., 2011; *Ménesguen et al*., 2012].

Geophysical fluid dynamics states that vortex dipoles steadily propagate eastward on the beta plane while single eddies propagate westward. Thus, dipoles that are generated near Portimão Canyon rotate to adopt an eastward-propagating configuration. This may explain the anticlockwise general motion in the Gulf of Cadiz. Once the dipoles are blocked against the topographic step at 8°W, they tend to rotate again or to split [see also *Carton et al*., 2002].

Again, this raises the question of the origin of the cyclonic circulation in the Gulf of Cadiz: is it due to the influence of the water mass exchange at Gibraltar [*Peliz et al*., 2009; *Lamas et al*., 2010], to that of the general circulation, or to the eddy field [*Alves et al*., 2011, this study]? In fact, all these studies point toward a strong three-dimensional coupling of motions in the Gulf of Cadiz. Presently, this coupling cannot be easily quantified because existing data sets lack synopticity and duration, and because numerical models do not yet fully reproduce the turbulent field in the Gulf. More complete data sets, perhaps relying on a large number of profiling floats and gliders, and very high-resolution numerical models, should be able to quantify more precisely the role of each effect in this cyclonic circulation and in its variability.

Acknowledgments
Thanks are due to SHOM (French Navy Hydrographic and Oceanographic Service) and to the Captain and Crew of R/V D'Entrecasteaux for data collection and processing. We acknowledge use of MedTop for data collection and processing. This study is part of the Semane research program funded by SHOM, DGA, IFREMER, and UBO. Portuguese Fundação para a Ciência e a Tecnologia is acknowledged for financial support of the MedTop Project.

References

Alves, J. M. R., X. Carton, and I. Ambar (2011), Hydrological structure, circulation and water mass transport in the Gulf of Cadiz, *Int. J. Geosci.*, *2*(4), 432–456.
Ambar, I. (1983), A shallow core of Mediterranean water off western Portugal, *Deep Sea Res., Part A*, *30*, 677–680.
Ambar, I., N. Serra, F. Neves, and T. Ferreira (2008), Observations of the Mediterranean Undercurrent and eddies in the Gulf of Cadiz during 2001, *J. Mar. Syst.*, *71*, 195–220.
Arhan, M., and A. Colin de Verdière (1985), Dynamics of eddy motions in the eastern north Atlantic, *J. Phys. Oceanogr.*, *15*, 153–170.
Armi, L., and W. Zenk (1984), Large lenses of highly saline Mediterranean Water, *J. Phys. Oceanogr.*, *14*, 1560–1576.
Armi, L., D. Hebert, N. Oakey, J. F. Price, P. L. Richardson, H. T. Rossby, and B. Ruddick (1989), Two years in the life of a Mediterranean salt lens, *J. Phys. Oceanogr.*, *19*, 354–370.
Barbosa Aguiar, A. C., A. Peliz, and X. Carton (2013), A census of Meddies in a long-term high-resolution simulation, *Prog. Oceanogr.*, *116*, 80–94.
Bashmachnikov, I., D. Boutov, and J. Dias (2013), Manifestation of two meddies in altimetry and sea-surface temperature, *Ocean Sci.*, *9*(2), 249–259.
Boebel, O., J. Lutjeharms, C. Schmid, W. Zenk, T. Rossby, and C. Barron (2003), The Cape Cauldron: A regime of turbulent inter-ocean exchange, *Deep Sea Res., Part II*, *50*(1), 57–86.
Bower, A. S. (1994), Meddies, eddies, floats and boats: "How do Mediterranean and Atlantic waters mix?", *Oceanus*, *37*, 12–15. [Available at http://findarticles.com/p/articles/mi_hb3324/is_n1_v37/ai_n28641434/.]
Bower, A. S., L. Armi, and I. Ambar (1995), Direct evidence of meddy formation off the southwestern coast of Portugal, *Deep Sea Res., Part I*, *42*, 1621–1630.
Bower, A. S., L. Armi, and I. Ambar (1997), Lagrangian observations of meddy formation during a Mediterranean undercurrent seeding experiment, *J. Phys. Oceanogr.*, *27*, 2545–2575.
Carton, X., L. Chérubin, J. Paillet, Y. Morel, A. Serpette, and B. Le Cann (2002), Meddy coupling with a deep cyclone in the Gulf of Cadiz, *J. Mar. Syst.*, *32*, 13–42.

Carton, X., N. Daniault, J. Alves, L. Chérubin, and I. Ambar (2010), Meddy dynamics and interaction with neighboring eddies southwest of Portugal: Observations and modeling, *J. Geophys. Res.*, *115*, C06017, doi:10.1029/2009JC005646.
Carton, X., M. Sokolovskiy, C. Ménesguen, A. Aguiar, and T. Meunier (2014), Vortex stability in a multi-layer quasi-geostrophic model: Application to Mediterranean Water eddies, *Fluid Dyn. Res.*, in press.
Chérubin, L., X. Carton, J. Paillet, Y. Morel, and A. Serpette (2000), Instability of the Mediterranean Water undercurrents southwest of Portugal: Effects of baroclinicity and of topography, *Oceanol. Acta*, *23*, 551–573.
Colin de Verdière, A. (1992), On the southward motion of Mediterranean salt lenses, *J. Phys. Oceanogr.*, *22*, 413–420.
Creswell, G. R. (1982), The coalescence of two East-Australian current warm-core eddies, *Science*, *215*, 161–164.
Cushman Roisin, B. (1989), On the role of filamentation in the merging of anticyclonic lenses, *J. Phys. Oceanogr.*, *19*, 253–258.
Daniault, N., J. P. Mazé, and M. Arhan (1994), Circulation and mixing of the Mediterranean water west of the Iberian Peninsula, *Deep Sea Res., Part I*, *41*, 1685–1714.
Dritschel, D. G. (2002), Vortex merger in rotating stratified flows, *J. Fluid Mech.*, *455*, 83–101.
Käse, R. H., and W. Zenk (1986), Reconstructed Mediterranean salt lens trajectories, *J. Phys. Oceanogr.*, *17*, 158–163.
Käse, R. H., A. Beckmann, and H. H. Hinrichsen (1989), Observational evidence of salt lens formation in the Iberian basin, *J. Geophys. Res.*, *94*, 4905–4912.
Käse, R. H., H. H. Hinrichsen, and T. Sanford (1996), Inferring density from temperature via a density-ratio relation, *J. Atmos. Oceanic Technol.*, *13*, 1202–1208.
Lamas, L., A. Peliz, I. Ambar, A. Barbosa Aguiar, N. Maximenko, and A. Teles-Machado (2010), Evidence of time-mean cyclonic cell southwest of Iberian Peninsula: The Mediterranean Outflow-driven beta-plume?, *Geophys. Res. Lett.*, *37*, L12606, doi:10.1029/2010GL043339.
Lamb, H. (1993), *Hydrodynamics*, chap. 7, 6th ed., 768 pp., Cambridge Univ. Press, Cambridge, U. K.
Madelain, F. (1970), Influence de la topographie de fond sur l'écoulement méditerranéen entre le détroit de Gibraltar et le cap Saint Vincent, *Cah. Oceanogr.*, *22*, 43–61.
Ménesguen, C., B. L. Hua, X. Carton, F. Klingelhöfer, and P. Schnürle (2012), Arms winding around a Meddy seen in seismic reflection data south of the Azores front, *Geophys. Res. Lett.*, *39*, L05604, doi:10.1029/2011GL050798.
Paillet, J., B. Le Cann, A. Serpette, Y. Morel, and X. Carton (1999), Real-time tracking of a northern meddy in 1997–98, *Geophys. Res. Lett.*, *26*, 1877–1880.
Paillet, J., B. Le Cann, X. Carton, Y. Morel, and A. Serpette (2002), Dynamics and evolution of a northern meddy, *J. Phys. Oceanogr.*, *32*, 55–79.
Peliz, A., P. Marchesiello, J. Dubert, A. Teles-Machado, M. Marta-Almeida, and B. Le Cann (2009), Surface circulation in the Gulf of Cadiz. Part 2: Inflow/outflow coupling and the Gulf of Cadiz Slope Current, *J. Geophys. Res.*, *114*, C03011, doi:10.1029/2008JC004771.
Prater, M. D., and T. B. Sanford (1994), A meddy of Cape St Vincent. Part I: Description, *J. Phys. Oceanogr.*, *24*, 1572–1586.
Quentel, E., X. Carton, and M. A. Gutscher (2011), Structure and temporal variability of Mediterranean Water from hydrological and marine seismic data south of Portimao Canyon (Gulf of Cadiz) from 1999 to 2002, *Int. J. Geosci.*, *2*(3), 185–194.
Richardson, P. L., and A. Tychensky (1998), Meddy trajectories in the Canary basin measured during the SEMAPHORE experiment, 1993–1995, *J. Geophys. Res.*, *103*, 25,029–25,045.
Richardson, P. L., D. Walsh, L. Armi, M. Schröder, and J. F. Price (1989), Tracking three meddies with SOFAR floats, *J. Phys. Oceanogr.*, *19*, 371–383.
Richardson, P. L., M. S. Mc Cartney, and C. Maillard (1991), A search for Meddies in historical data, *Dyn. Atmos. Oceans*, *15*, 241–265.
Richardson, P. L., A. S. Bower, and W. Zenk (2000), A census of meddies tracked by floats, *Progr. Oceanogr.*, *45*, 209–250.
Sadoux, S., J. M. Baey, A. Fincham, and D. Renouard (2000), Experimental study of the stability of an intermediate current and its interaction with a cape, *Dyn. Atmos. Oceans*, *31*, 165–192.
Schultz-Tokos, K., H. H. Hinrichsen, and W. Zenk (1994), Merging and migration of two meddies, *J. Phys. Oceanogr.*, *24*, 2129–2141.
Serra, N., and I. Ambar (2002), Eddy generation in the Mediterranean undercurrent, *Deep Sea Res., Part II*, *49*, 4225–4243.
Serra, N., I. Ambar, and R. H. Käse (2005), Observations and numerical modeling of the Mediterranean Outflow splitting and eddy generation, *Deep Sea Res., Part II*, *52*, 383–408.
Serra, N., I. Ambar, and D. Boutov (2010), Surface expression of Mediterranean Water dipoles and their contribution to the shelf/slope—Open ocean exchange, *Ocean Sci.*, *6*, 191–209.
Shapiro, G. I., and S. L. Meschanov (1996), Spreading pattern and mesoscale structure of Mediterranean outflow in the Iberian Basin estimated from historical data, *J. Mar. Syst.*, *7*, 337–348.
Song, H., L. M. Pinheiro, B. Ruddick, and F. C. Teixeira (2011), Meddy, spiral arms, and mixing mechanisms viewed by seismic imaging in the Tagus Abyssal Plain (SW Iberia), *J. Mar. Res.*, *69*, 827–842.
Tychensky, A., and X. J. Carton (1998), Hydrological and dynamical characterization of meddies in the Azores region: A paradigm for baroclinic vortex dynamics, *J. Geophys. Res.*, *103*, 25,061–25,079.
Van Heijst, G. J. F., and J. B. Flor (1989), Dipole formation and collisions in a stratified fluid, *Nature*, *340*, 212–215.
Velasco Fuentes, O. U., and G. J. F. Van Heijst (1995), Collision of dipolar vortices on a β plane, *Oceanogr. Lit. Rev.*, *43*(7), 2735–2750.
Zenk, W. (1975), On the Mediterranean outflow west of Gibraltar, *Meteor Forschungsergeb., Reihe A*, *16*, 15–22.
Zenk, W., K. L. Schultz-Tokos, and O. Boebel (1992), New observations of meddy movement south of the Tejo plateau, *Geophys. Res. Lett.*, *12*, 2389–2392.